CHAPTER SIX

Genitourinary

URINARY TRACT INFECTIONS

Urinary tract infection (UTI) is the most common problem of the genitourinary system encountered in children. The urinary tract is the second most common site of infection in children overall, with the upper respiratory tract being the first. The incidence of UTI is higher in girls than in boys, probably because of the short length of the female urethra. There is some current controversy concerning when children with UTIs should be imaged. Most physicians would agree that boys should be studied after the first UTI and that girls should be studied after the second UTI. However, there are some physicians who advocate that all children should be imaged after the first UTI. The immediate goals of imaging children with UTIs include identifying underlying congenital anomalies that predispose the child to UTI, identifying vesicoureteral reflux, identifying and documenting any renal cortical damage, providing a baseline renal size for subsequent evaluation of renal growth, and establishing prognostic factors. The long-term goal is to eliminate the chance of renal damage leading to chronic renal disease and hypertension.

The workup of a child with a UTI typically involves both a renal ultrasound and a voiding cystourethrogram. Voiding cystourethrograms can be performed using fluoroscopy or nuclear medicine. There is some debate about the indications for one or the other of the two studies. The advantage of the fluoroscopic cystourethrogram is that it demonstrates better anatomic detail. The advantage of the nuclear cystogram is that the patient is exposed to less radiation. However, in modern fluoroscopic units with pulse fluoroscopy, the difference in radiation dose between the two techniques is minimal. Because of the need for sharp anatomic detail in all boys and in girls with anatomic abnormalities demonstrated on ultrasound, most would advocate fluoroscopic cystograms for those patients. Nuclear cystograms are adequate for girls with normal ultrasound examinations.

Renal Ultrasound

At Cincinnati Children's Hospital Medical Center, renal ultrasounds are performed with the patient both in the supine and the prone positions. Transverse and longitudinal images are obtained of the kidney and bladder. Renal lengths are measured in both the prone and supine positions but are often more accurate with the patient in the prone position. In every case, it is important to compare the patient's renal length with tables that plot normal renal length against age. Also, the left and right kidneys should normally be within 1 cm of each other. If there is a discrepancy of more than 1 cm, an underlying abnormality should be suspected. A size discrepancy may result from a disorder that causes one of the kidneys to be too small, such as global scarring, or from a process that causes one of the kidneys to be too large, such as acute pyelonephritis or renal duplication.

The kidneys of infants have several characteristics that are different from those of older children and adults. They commonly have a prominent undulating contour. This is a normal appearance secondary to fetal lobulation (Fig. 6-1). In addition, infants' kidneys can demonstrate prominent hypoechoic renal pyramids (see Fig. 6-1) in contrast to the more echogenic renal cortex. These findings should not be mistaken for hydronephrosis.

Fluoroscopic Voiding Cystourethrogram

The most common indication for a fluoroscopic voiding cystourethrogram (VCUG) is the evaluation of UTI. Other indications include voiding dysfunction, enuresis, and the workup for hydronephrosis. The VCUG demonstrates the presence or absence of vesicoureteral reflux and also documents anatomic abnormalities of the bladder and urethra. Because catheterization is used for the procedure, there can be a great deal of anxiety for both the patient and the parents. Education of the parents and patient prior to

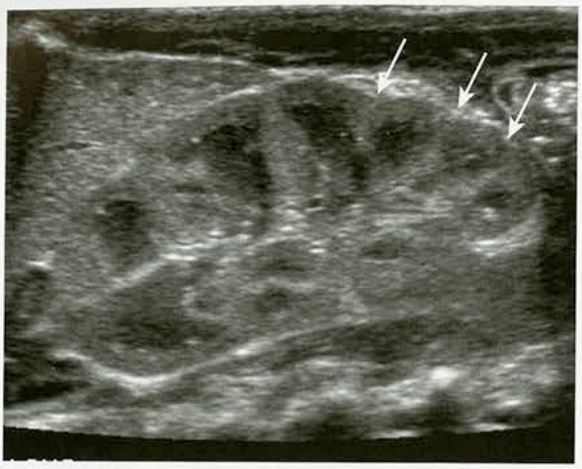

FIGURE 6-1. Normal ultrasound appearance of neonatal kidney. Longitudinal ultrasound shows prominent hypoechoic renal pyramids. This normal finding should not be confused with hydronephrosis. Also note fetal lobulation as focal indentations *(arrows)* located between medullary pyramids.

the examination is crucial to optimizing the patient's experience. VCUGs are performed under fluoroscopy with the patient awake. The patient is catheterized under sterile conditions on the fluoroscopy table, typically using an 8F catheter. A precontrast scout view of the abdomen is usually obtained to evaluate for calcifications, to document the bowel pattern so that it is not later mistaken for vesicoureteral reflux, and to document the catheter position within the bladder. Contrast is then instilled into the bladder. An early filling view of the bladder should be obtained to exclude a ureterocele. A ureterocele appears as a round, well-defined filling defect on early filling views. On later full views of the bladder, a ureterocele can be compressed and obscured. Once the patient's bladder is full, bilateral oblique views are obtained to visualize the regions of the ureteral vesicular junctions. These views are typically obtained with the collimators open from top to bottom, with the bladder positioned at the inferior aspect of the screen and the expected path of the ureter included on the film. During voiding, the male urethra is optimally imaged with the patient in the oblique projection. The female urethra is best seen on the anteroposterior view. It is critical to obtain an image of the urethra during voiding, particularly in males. In order to ensure that a view of the urethra is obtained, an image should be obtained during urination with the catheter in place and then a second view can be obtained after the catheter has been removed. After the patient has completed voiding, images are obtained of the pelvis and over the kidneys, documenting the presence or absence of vesicoureteral reflux and evaluating the extent of postvoid residual contrast within the bladder. The use of fluoroscopy should be brief and intermittent during bladder filling. Fluoroscopic last-image hold images can often substitute for true exposures in order to further decrease radiation dose.

Sometimes, particularly in older children, it may be difficult to get the child to void on the table. Almost all children will eventually void and a great deal of patience is required during such prolonged examinations. There are several maneuvers that may help the child to void. They include placing warm water on the patient's perineum or toes; placing a warm, wet washcloth on the patient's lower abdomen; tilting the table so that the head is up; letting the patient hear the sound of running water in the sink; and dimming the lights.

The expected bladder capacity of small children can be calculated by adding 2 to the patient's age in years and multiplying that number by 30. This yields the bladder capacity in milliliters. Obviously, this formula works only up to a certain age.

Acute Pyelonephritis

There is some confusion concerning the terminology used for infections of the urinary tract in children. The definition of UTI is the presence of bacteria in the urine, but the term typically refers to infections of the lower urinary tract. Acute pyelonephritis is defined as urinary tract infection that involves the kidney. Young children may present with nonspecific symptoms, such as fever, irritability, and vague abdominal pain. In older children, the findings may be more specific, such as fever associated with flank pain. In patients in whom the diagnosis is straightforward, no imaging is needed during the acute infection, but the patients are imaged later as the standard workup for UTI. In patients in whom there is clinical difficulty in distinguishing an upper from a lower UTI, cortical scintigraphy using dimercaptosuccinic acid (DMSA) has been advocated as being the most sensitive test. In the case of pyelonephritis, this study demonstrates single or multiple areas of lack of renal uptake of the radiotracer. These areas tend to be triangular and peripheral (Fig. 6-2). Other imaging studies

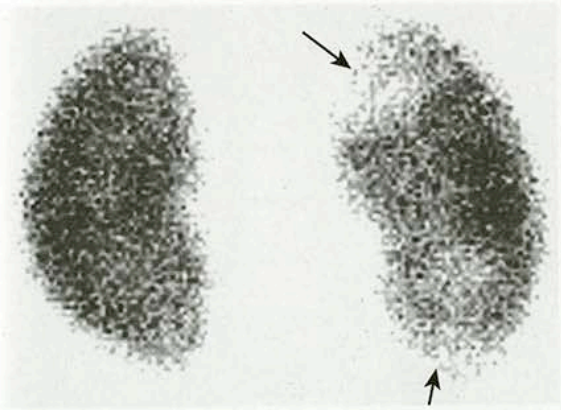

FIGURE 6-2. Acute pyelonephritis. Nuclear scintigraphy with dimercaptosuccinic acid (DMSA) shows areas of decreased uptake *(arrows)* in the upper and lower poles of the right kidney, consistent with pyelonephritis in a child with known reflux and flank pain.

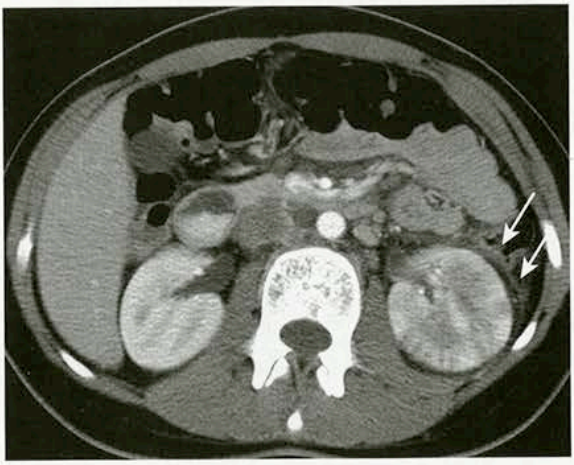

FIGURE 6-4. Acute pyelonephritis on CT obtained for abdominal pain. Pyelonephritis appears as asymmetric increased volume of left kidney, striated low attenuation within peripheral aspect of left kidney, and perinephric stranding with thickening of Gerota fascia *(arrows)*.

that have also been advocated to detect acute pyelonephritis include color Doppler ultrasound and contrast-enhanced helical computed tomography (CT). These studies typically demonstrate lack of color flow or contrast enhancement of triangular, peripheral portions of the kidney (Fig. 6-3). CT may show a striated nephrogram (Fig. 6-4). Also, pyelonephritis can be very focal and can mimic a mass on all of these studies (Fig. 6-5A, B). Ultrasound and CT may also demonstrate disproportionate enlargement and swelling of the affected kidney as compared to the contralateral side. Sometimes the findings of pyelonephritis will be encountered on these imaging studies when the studies were obtained for other suspected causes of abdominal pain such as appendicitis.

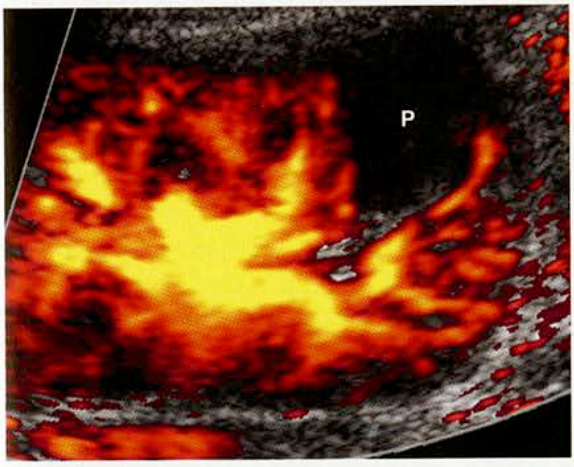

FIGURE 6-3. Acute pyelonephritis on Doppler ultrasound. Longitudinal ultrasound shows lesion (P) as peripheral area of absent color flow.

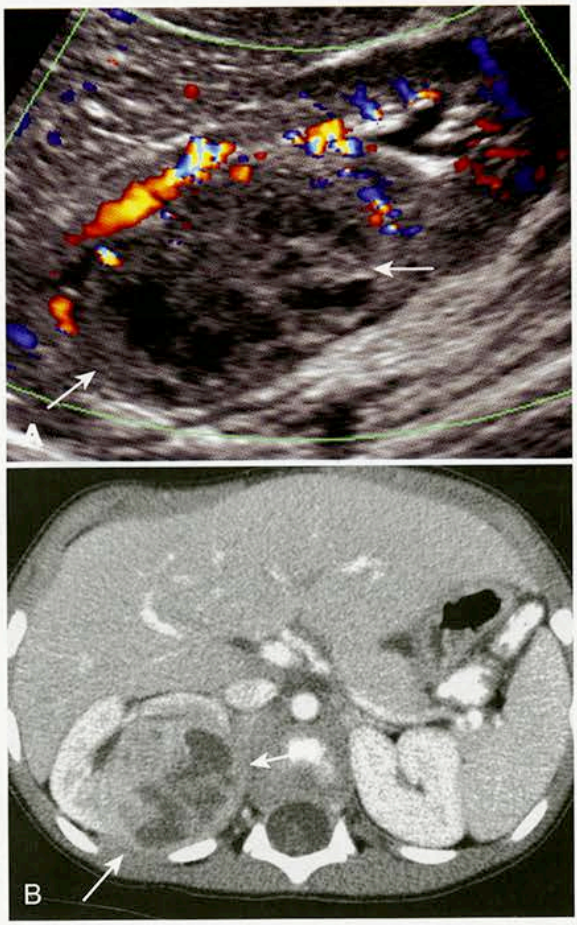

FIGURE 6-5. Acute, focal pyelonephritis presenting as a mass. **A,** Longitudinal ultrasound shows a heterogeneous mass *(arrows)* with areas of low echogenicity. **B,** CT shows heterogeneous mass *(arrows)* with low attenuation.

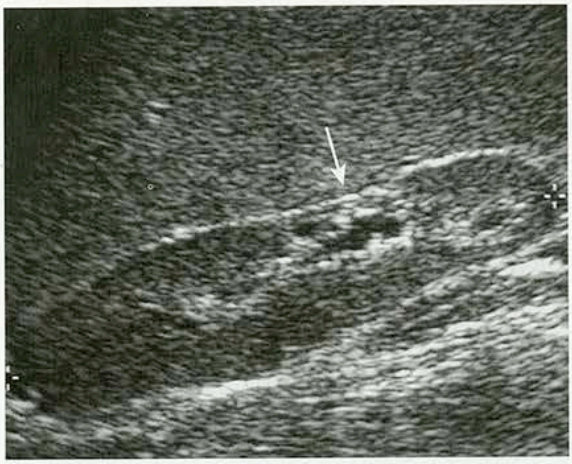

FIGURE 6-6. Global renal scarring shown on longitudinal ultrasound of the left kidney. There is diffuse thinning of the renal parenchyma, most striking in the lower pole *(arrow)*, where the renal surface is in close approximation to the collecting system.

Chronic Pyelonephritis

Chronic pyelonephritis is defined as the loss of renal parenchyma resulting from previous bacterial infection. It is synonymous with renal scarring. Normally, the renal cortical thickness should be symmetric and equal within the upper, mid, and lower poles of the kidneys. The loss of renal cortical substance as seen by ultrasound, most commonly at one of the renal poles, is suggestive of the diagnosis (Fig. 6-6). This should not be confused with fetal lobulation (also known as an interrenicular septum; Fig. 6-7A, B), a normal variant. In pyelonephrotic scarring, the indentations of the renal contour tend to overlie the renal calyces, whereas in fetal lobulation, the indentations are between renal calyces (see Fig. 6-7).

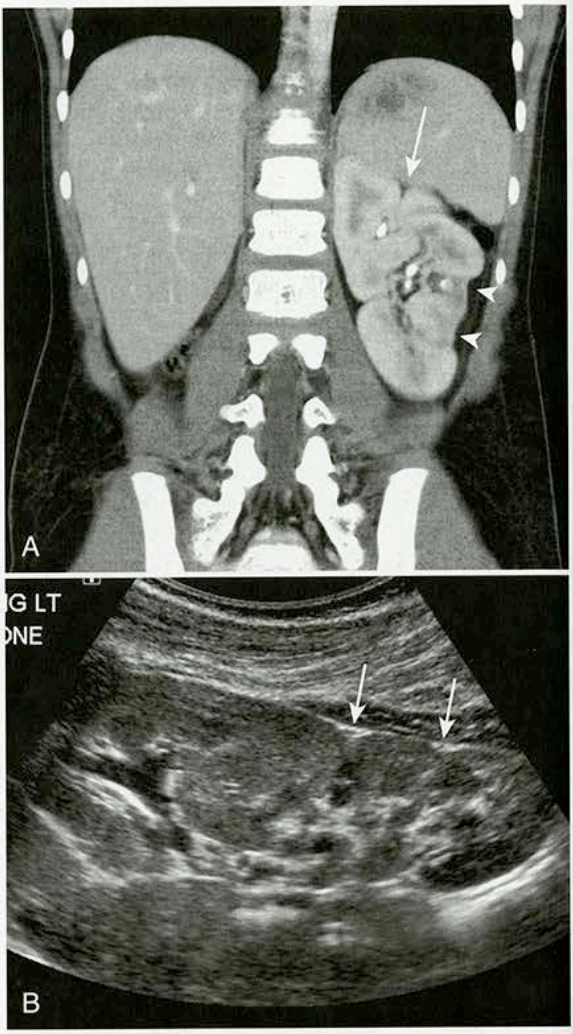

FIGURE 6-7. Differentiation between fetal lobulation and focal scarring; both are demonstrated in the same patient with a solitary left kidney. **A,** Coronal CT shows solitary left kidney. There are indentations of the renal cortex directly over the medullary pyramids *(arrowheads)*. These areas represent focal scarring. There is also an indentation in the renal cortex between the medullary pyramids *(arrow)*. This is consistent with fetal lobulation. **B,** Longitudinal ultrasound in same patient again shows indentations of the renal cortex directly over the medullary pyramids *(arrows)*, which is consistent with focal scarring.

EVALUATION OF PRENATALLY DIAGNOSED HYDRONEPHROSIS

As a result of the increasing use of prenatal ultrasound, pediatric radiologists are more frequently having to perform postnatal workups of prenatally diagnosed hydronephrosis. The evaluation of such patients typically includes both ultrasound and VCUG. The controversy revolves around the timing of the ultrasound evaluation. In neonates, there is a relative state of dehydration that occurs after the first 24 hours of life. Reports have shown that this relative state of dehydration can lead to underestimation or nondetection of hydronephrosis by ultrasound. Therefore, it is recommended that the postnatal evaluation of prenatally diagnosed hydronephrosis be performed during the first 24 hours of life or after 1 week of age. The disadvantage of doing the ultrasound during the first 24 hours of life is the interruption of mother-child bonding, whereas the disadvantage of performing the examination at 7 days of life is the potential of parental noncompliance and losing the patient for follow-up.

Congenital Anomalies

Congenital anomalies of the genitourinary tract are commonly encountered during workups for UTIs or other abnormalities.

Vesicoureteral Reflux

Vesicoureteral reflux (VUR) is defined as retrograde flow of urine from the bladder into the ureter. It is thought to be a primary abnormality related to immaturity or maldevelopment of the ureterovesicular junction. Normally, the ureter enters the ureterovesicular junction in an oblique manner such that the intramural ureter traverses the bladder wall for an adequate length to create a passive antireflux valve. When the angle of entrance of the ureter is abnormal, vesicoureteral reflux results. VUR occurs in less than 0.5% of asymptomatic children but is present in as much as 50% of children with UTIs. There is an increased incidence of VUR in siblings of children with VUR, in children of parents who had VUR, and in non-blacks as compared to blacks. The importance of VUR is its association with renal parenchymal scarring. VUR is present in almost all children with severe renal scarring. Also, a direct correlation between the grade of VUR and the prevalence of scarring has been demonstrated. Other complications associated with VUR include acute pyelonephritis, interference with the normal growth of the kidney, and development of hypertension. The degree of VUR is graded on the basis of several characteristics (Fig. 6-8): the level to which the reflux occurs (ureteral vs. ureteral and collecting system); the degree of dilatation; the calyceal blunting; and papillary impressions. Grade 1 reflux is confined to the ureter. Grade 2 reflux fills the ureter and collecting system, but there is no dilatation of the collecting system. Grade 3 reflux is associated with blunting of the calyces. In deciding whether a calyx is dilatated or not, I was taught that if it looks like you could pick your teeth with a calyx, it is not dilatated (Fig. 6-9). Grade 4 reflux is identified by progressive, tortuous dilatation of the renal collecting system. Grade 5 reflux is defined by the presence of a very tortuous dilatated ureter. Both grade 4 and grade 5 reflux can be associated with intrarenal reflux. It is surprising, but significant VUR can be present in spite of a normal renal ultrasound. Lack of dilatation on ultrasound in no way excludes the presence of VUR. Dilatation of the ureter or collecting systems can sometimes be seen intermittently when VUR is present.

Most low-grade VUR resolves spontaneously by the age of 5 to 6 years unless there is an underlying anatomic abnormality. In children without anatomic reasons that prohibit spontaneous resolution of reflux, most are

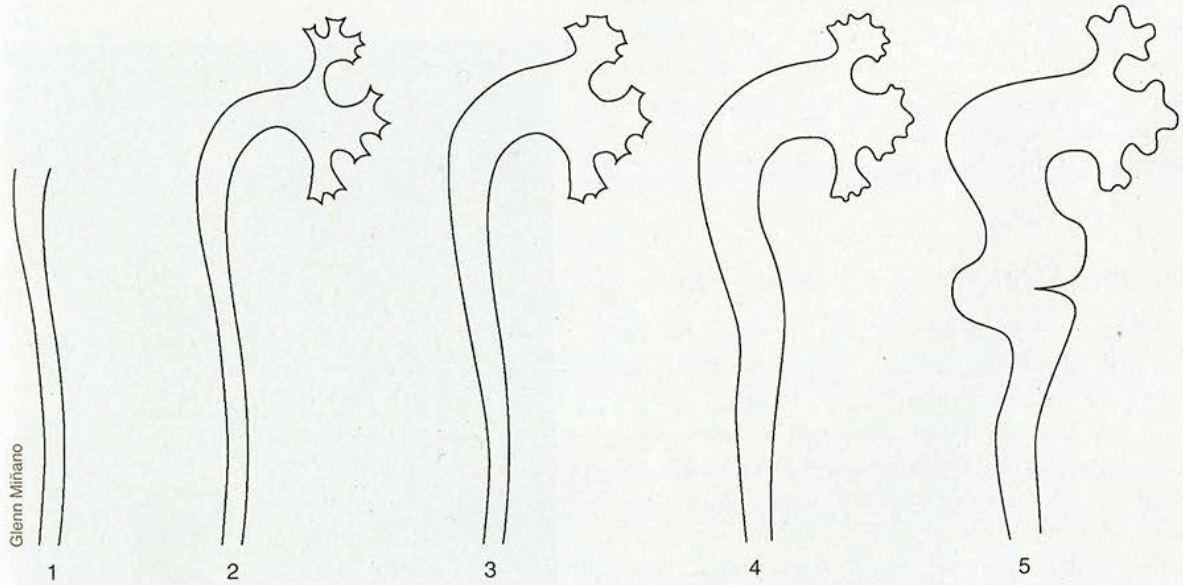

FIGURE 6-8. Grading system for vesicoureteral reflux. Grade 1 Reflux is confined to the ureter. Grade 2: Reflux fills the ureter and collecting system without dilatation of the collecting system. Grade 3: Reflux is associated with blunting of the calyces. Grade 4: Reflux results in progressive, tortuous dilatation of the renal collecting system. Grade 5: Reflux is defined by the presence of a very tortuous, dilatated ureter.

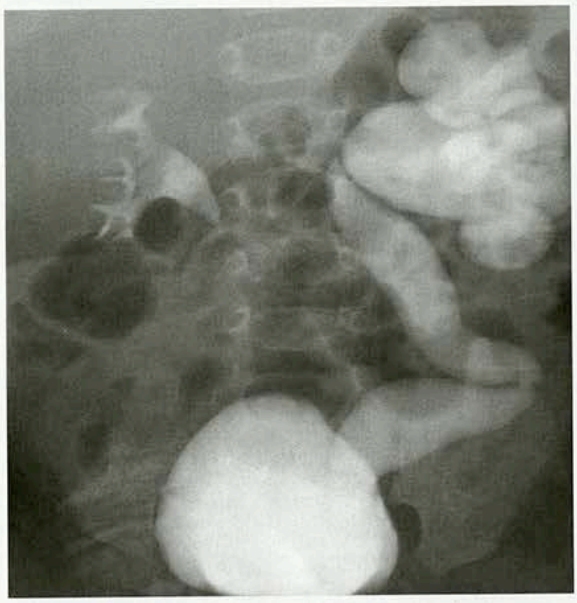

FIGURE 6-9. Vesicoureteral reflux shown on voiding cystourethrogram: right, grade 2, and left, grade 5. Image shows reflux of contrast filling a nondilatated right renal collecting system. Note that the calyces are sharp in appearance and are not blunted. On the left, there is reflux of contrast filling a markedly dilated ureter and collecting system. The calyces are markedly blunted. The ureter is tortuous.

treated with prophylactic antibiotics alone. Antibiotic therapy is discontinued when the reflux has resolved. Surgical reimplantation of the ureter or periureteral injection (minimally invasive endoscopic treatment) is considered when the degree of VUR is severe, if there is evidence of renal scarring, if the VUR has not resolved over a reasonable time, or if breakthrough infections occur frequently. After periureteral injection, ultrasound will show an echogenic mound in the bladder wall in the region of the treated ureteral orifice (Fig. 6-10).

Ureteropelvic Junction Obstruction

Ureteropelvic junction (UPJ) obstruction is defined as an obstruction of the flow of urine from the renal pelvis into the proximal ureter. It is the most common congenital obstruction of the urinary tract. There is an increased incidence of other congenital anomalies of the urinary tract in patients with UPJ obstruction. They include vesicoureteral reflux, renal duplication, and ureterovesicular junction obstruction. In addition, UPJ obstruction may be present bilaterally but the severity may be asymmetric. The cause of most UPJ obstructions is intrinsic

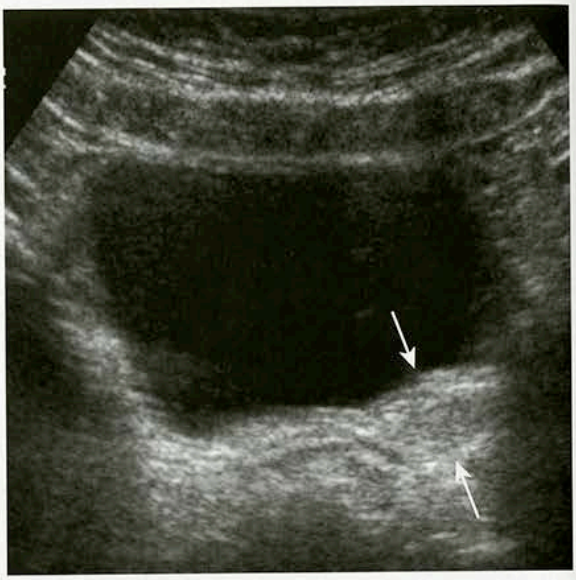

FIGURE 6-10. Ultrasound appearance following minimally invasive endoscopic treatment of VUR using periureteral injection of Deflux. Ultrasound shows echogenic mound *(arrows)* at base of bladder in region of left ureterovesicular junction.

narrowing at the UPJ. However, extrinsic compression secondary to anomalous vessels is also occasionally identified. On ultrasound, there is dilatation of the renal collecting system without dilatation of the ureter (Fig. 6-11). The degree of dilatation may be severe. Renal scintigraphy using 99m technetium-MAG3 with diuretic (furosemide) challenge is often used to evaluate the severity of the UPJ obstruction. Children with

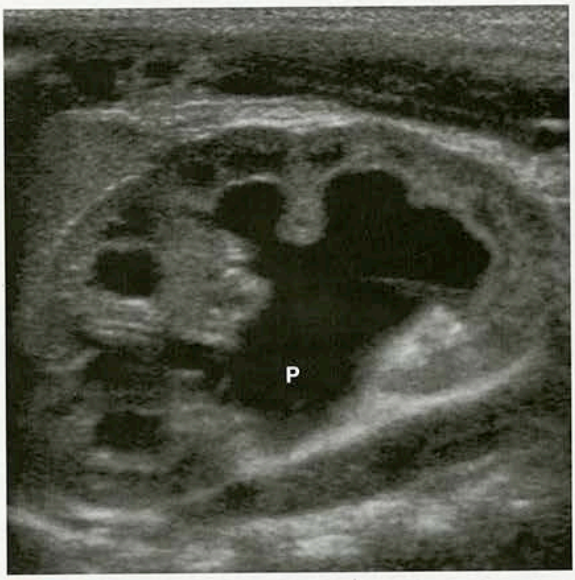

FIGURE 6-11. UPJ obstruction. Longitudinal ultrasound shows dilatation of renal collecting system, which connects to central, dilatated renal pelvis *(P)*. The ureter was not dilatated.

FIGURE 6-12. Renal injury to child with UPJ obstruction following minor trauma. CT shows findings of UPJ obstruction with dilatation of the renal collecting system and central, dilatated renal pelvis *(P)*. There is a large amount of perinephric fluid secondary to injury to the dilatated collecting system.

UPJ obstruction and other congenital anomalies are predisposed to renal injury even by minor abdominal trauma (Fig. 6-12). Mild to moderate UPJ obstructions are sometimes treated conservatively, but most urologists treat severe UPJ obstruction surgically.

Multicystic Dysplastic Kidney

Multicystic dysplastic kidney (MCDK) is thought to be related to severe obstruction of the renal collecting system during fetal development. The site of the obstruction determines the imaging appearance. The most common appearance of MCDK is that of a grapelike collection of variably sized cysts that do not appear to communicate (Fig. 6-13). The absence of a central dominant cyst differentiates MCDK from severe hydronephrosis. However, if the level of the fetal obstruction is within the proximal ureter, the "hydronephrotic" form of MCDK can occur; in this there is a central pelvis surrounded by dilatated cysts. In such cases, renal scintigraphy can be useful in differentiating severe UPJ obstruction from MCDK. In MCDK, no trace or accumulation is seen within the renal pelvis on 4-hour images. In patients with MCDK, it is important to exclude other associated congenital anomalies of the contralateral kidney. UPJ obstruction is

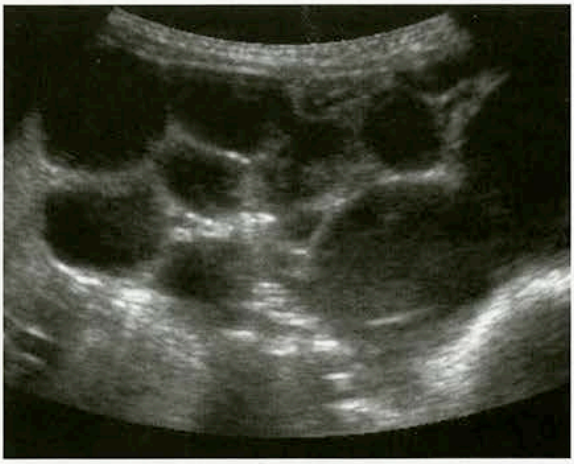

FIGURE 6-13. Multicystic dysplastic kidney shown on longitudinal ultrasound as cluster of anechoic cysts without dominant central cyst. Scintigraphy showed no renal activity.

commonly identified. Rarely, MCDK can be isolated to an upper or lower pole.

Most MCDKs slowly decrease in size over time. Often the remaining residual dysplastic renal tissue will no longer be visualized by imaging techniques. Although in the past, nephrectomy was the usual treatment for MCDK, most patients are currently treated nonoperatively. They are, however, followed by ultrasound because there is some controversy as to whether there may be an increased risk for developing malignancy in an MCDK. MCDK can also predispose patients to hypertension, and if hypertension develops, nephrectomy is usually performed.

Ureteropelvic Duplications

The term *ureteropelvic duplication* refers to a broad range of anatomic variations ranging in severity from incomplete to complete. The incomplete form of duplication is more common than the complete form. With incomplete duplication, there can be a bifid renal pelvis, two ureters superiorly that join in midureter, or duplicated ureters that join just prior to insertion into the bladder wall. With complete duplication there are two completely separate ureters that have separate orifices into the bladder. Ureteropelvic duplication is thought to occur secondary to premature division or duplication of the ureteral bud. Such duplications are five times more common unilaterally than bilaterally. On ultrasound, incomplete renal duplication may appear as an area of echogenicity similar to the renal cortex separating the echogenic central renal fat into superior and inferior

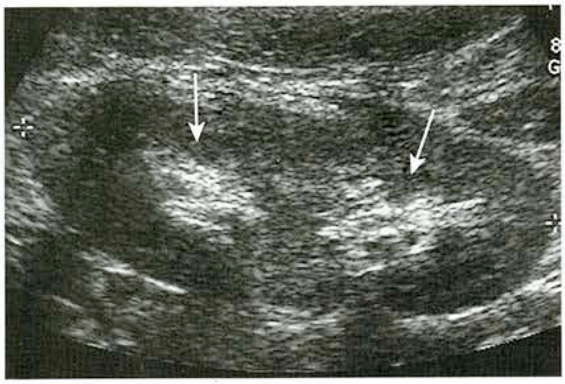

FIGURE 6-14. Intrarenal duplication shown on longitudinal ultrasound as an area of echogenicity similar to that of the renal cortex separating the central pelvicalyceal fat into separate superior and inferior components *(arrows)*.

components (Fig. 6-14). Noncomplicated, incomplete renal duplications have little significance and should be thought of as a normal variation. Children with incomplete duplication are not at increased risk for urinary tract disease as compared to children without duplications.

In patients with complete ureteropelvic duplication, there is a higher incidence of urinary tract infection, obstruction, vesicoureteral reflux, and parenchymal scarring. In these patients the ureteral orifice of the upper pole moiety inserts more medially and more inferiorly than the orifice of the lower pole ureter. This is known as the Weigert-Meyer rule. The lower pole system is more prone to vesicoureteral reflux and UPJ obstruction. The upper pole system is more prone to obstruction secondary to ureterocele (Figs. 6-15A-C, 6-16A, B).

Ureterocele

A ureterocele is defined as dilatation of the distal ureter. The dilatated portion of the ureter lies between the mucosal and muscular layers of the bladder. The ureteral orifice is usually stenotic or obstructed. Ureteroceles are defined as simple when they are positioned at the expected orifice of the ureter at the lateral aspect of the trigone; they are defined as ectopic when they are associated with an ectopic insertion of the ureter. Ectopic ureteroceles can be quite large

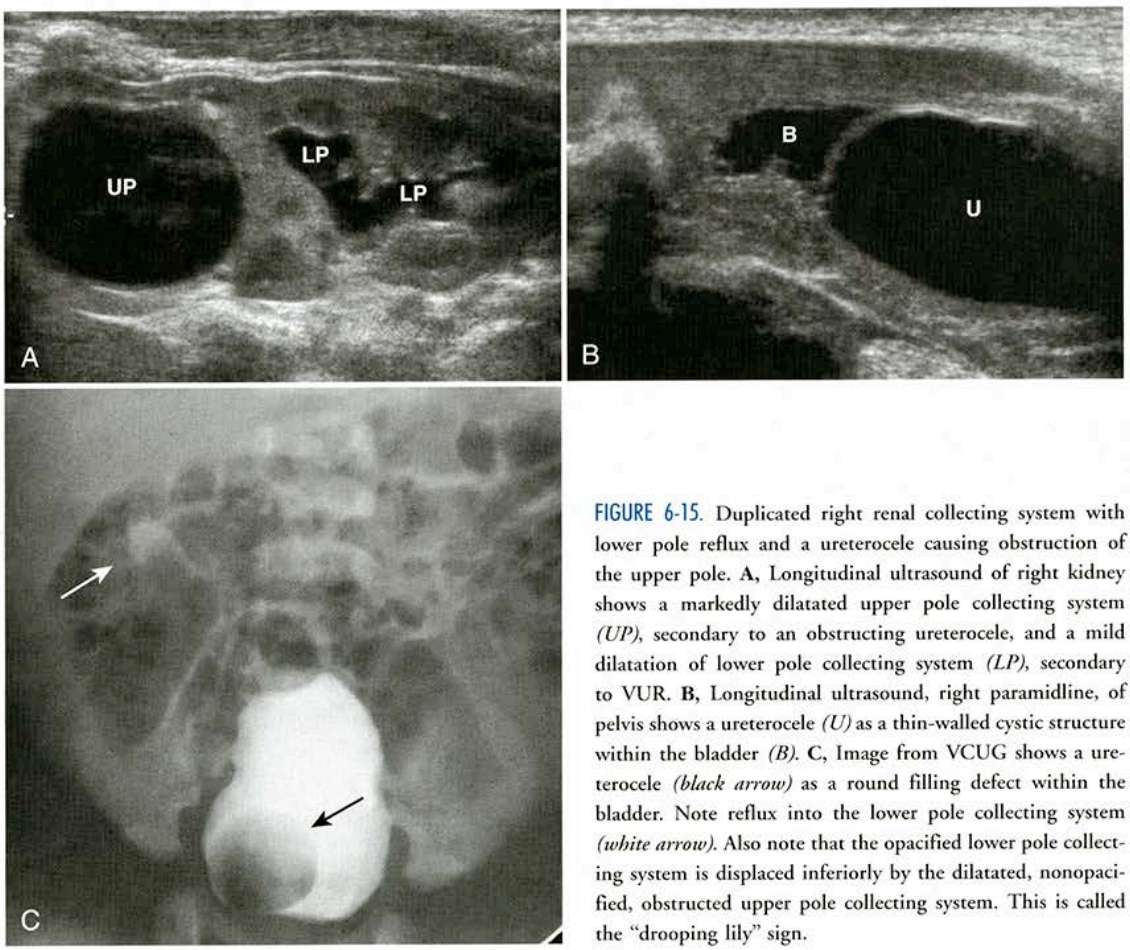

FIGURE 6-15. Duplicated right renal collecting system with lower pole reflux and a ureterocele causing obstruction of the upper pole. **A,** Longitudinal ultrasound of right kidney shows a markedly dilatated upper pole collecting system *(UP)*, secondary to an obstructing ureterocele, and a mild dilatation of lower pole collecting system *(LP)*, secondary to VUR. **B,** Longitudinal ultrasound, right paramidline, of pelvis shows a ureterocele *(U)* as a thin-walled cystic structure within the bladder *(B)*. **C,** Image from VCUG shows a ureterocele *(black arrow)* as a round filling defect within the bladder. Note reflux into the lower pole collecting system *(white arrow)*. Also note that the opacified lower pole collecting system is displaced inferiorly by the dilatated, nonopacified, obstructed upper pole collecting system. This is called the "drooping lily" sign.

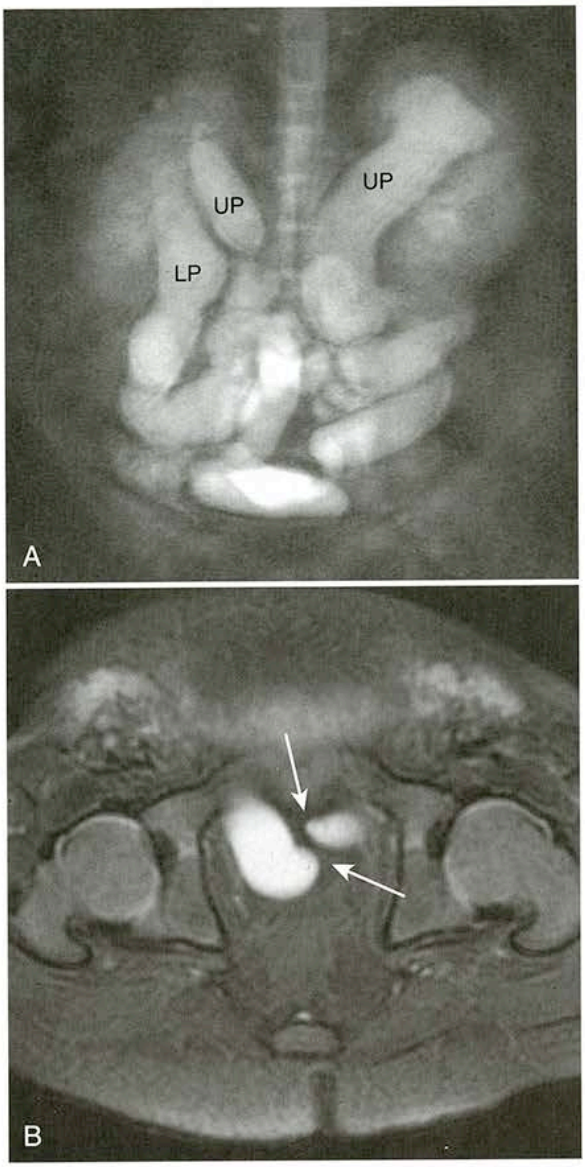

FIGURE 6-16. Complex bilateral duplication shown on an MRI urogram. **A,** MRI urogram shows marked dilatation of the upper pole collecting systems and ureters *(UP)* bilaterally, secondary to obstruction by ectopic ureter insertion. The right lower pole collecting system and ureter *(LP)* is also dilatated secondary to VUR. **B,** Axial T2-weighted MR image shows ectopic low-inserting bilateral ureters *(arrows)*. Both ureters insert into the urethra below the bladder base.

and are almost always associated with a duplicated collecting system (see Figs. 6-15, 6-16). The ureter from the upper pole moiety is associated with the ureterocele. There can be marked associated dilatation of that ureter and the upper pole moiety collecting system. On VCUGs, ureteroceles appear as round, well-defined filling defects, best visualized on early filling views (see Fig. 6-15). Ureteroceles may be compressed and not visualized when the bladder is distended by contrast. Sometimes the ureteroceles can invert and appear as diverticula. On ultrasound, typically a dilatated ureter is seen to terminate in a round, anechoic intravesicular cystic structure (see Fig. 6-15). Usually there is associated dilatation of the upper pole moiety.

Renal Ectopia and Fusion

Renal ectopia is defined as abnormal position of the kidney. It results from abnormal migration of the kidney from its fetal position within the pelvis to its expected position in the renal fossa. Most ectopic kidneys lie within the pelvis and are malrotated. Renal fusion is defined as a connection between the two kidneys. It results from failure of separation of the primitive nephrogenic cell masses into two separate left and right blastemas. With ectopia, the ectopic kidney most commonly lies within the pelvis. Most ectopic kidneys are also malrotated. With cross-fused renal ectopia, both kidneys lie on the same side of the abdomen and are fused (Fig. 6-17). The ureter from the ectopic kidney crosses the midline and enters the bladder in the expected location of the contralateral ureterovesicular junction. The most common type of renal fusion is horseshoe kidney, which occurs in approximately 1 in 600 births. With horseshoe kidney, there is fusion of the lower

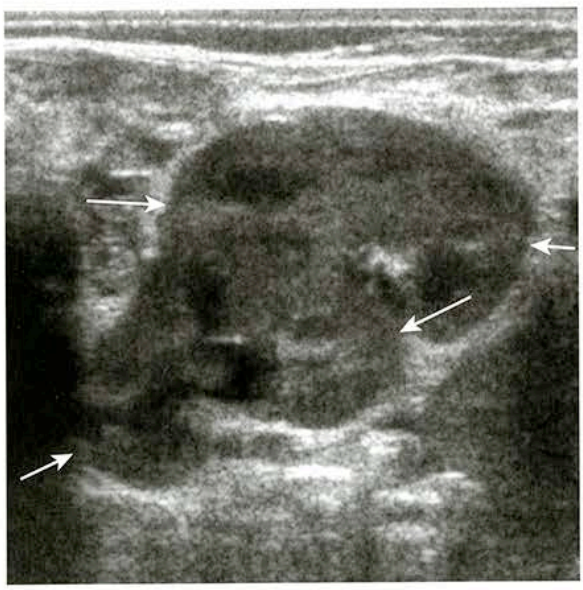

FIGURE 6-17. Crossed-fused renal ectopia is demonstrated as fusion of the "left" and right kidneys to the right of the midline on ultrasound. The *arrows* point to the upper and lower poles of the two kidney units.

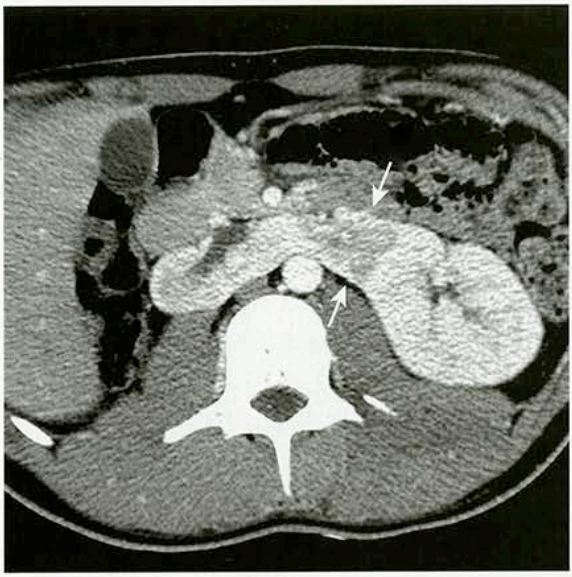

FIGURE 6-18. CT of horseshoe kidney with contusion due to a minor injury. There is an area of low attenuation *(arrows)* within the horseshoe kidney, consistent with a contusion.

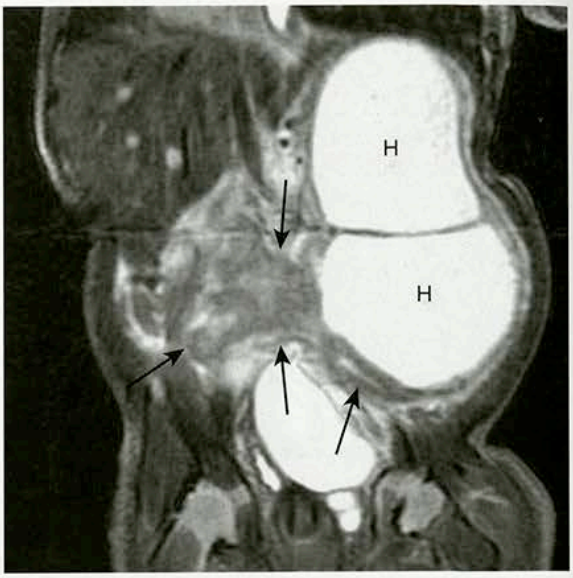

FIGURE 6-19. Horseshoe kidney with associated left hydronephrosis. Coronal T2-weighted MRI shows horseshoe kidney *(arrows)* with a parenchymal connection of the kidneys across the midline. Note hydronephrosis *(H)* of the left renal moiety.

pole of the two kidneys across the midline. The connecting isthmus may consist of functional renal tissue or fibrous tissue and cross the midline anterior to the aorta and inferior vena cava. Most horseshoe kidneys are located more inferiorly than normal. The number of ureters arising from a horseshoe kidney is variable and they exit the kidney ventrally rather than ventromedially. Horseshoe kidneys and other types of renal fusions are at increased risk for infection, injury from mild traumatic events (Fig. 6-18), renal vascular hypertension, stone formation, and hydronephrosis (Fig. 6-19); there is also a slight increase in incidence of Wilms tumor and adenocarcinoma. On ultrasound, horseshoe kidney may be difficult to diagnose on the standard longitudinal and axial planes. It may also be difficult to obtain accurate measurements of the kidneys in the longitudinal plane because of the poorly defined inferior pole. If the ultrasound probe is moved posterolaterally and the patient is scanned in the coronal plane, the two kidneys and connecting isthmus can be visualized on a single image (Fig. 6-20A-C). Such images are most easily obtained in infants. Horseshoe kidneys are readily visualized on CT scanning (see Fig. 6-20).

Primary Megaureter

Primary megaureter can be thought of as the ureteral equivalent of Hirschsprung disease. With primary megaureter, there is an aperistaltic segment of the distal ureter that results in a relative obstruction (Fig. 6-21). The normal more proximal ureter dilates as a consequence of the relative obstruction. It is more common on the left and in boys. Children affected with primary megaureter may present with infection or be diagnosed prenatally. Ultrasound demonstrates hydronephrosis and enlargement of the ureter above the aperistaltic segment.

Posterior Urethral Valves

Posterior urethral valves are the most common cause of urethral obstruction in male infants. They are identified most commonly in infancy but can be diagnosed in older children. The high back pressure and associated reflux can damage the kidneys and result in renal failure. Affected children can be diagnosed prenatally and present with renal failure or with urinary tract infection.

Typical ultrasound features include a thick-walled bladder with associated bilateral dilatation of the renal collecting systems and ureters (Figs. 6-22A-D, 6-23A-C). Occasionally, a dilatated posterior urethra can be identified inferior to the bladder. On VCUG, the posterior urethra appears very dilatated (see Figs. 6-22, 6-23). The actual valve itself may be difficult to visualize but can appear as a membranelike obstruction

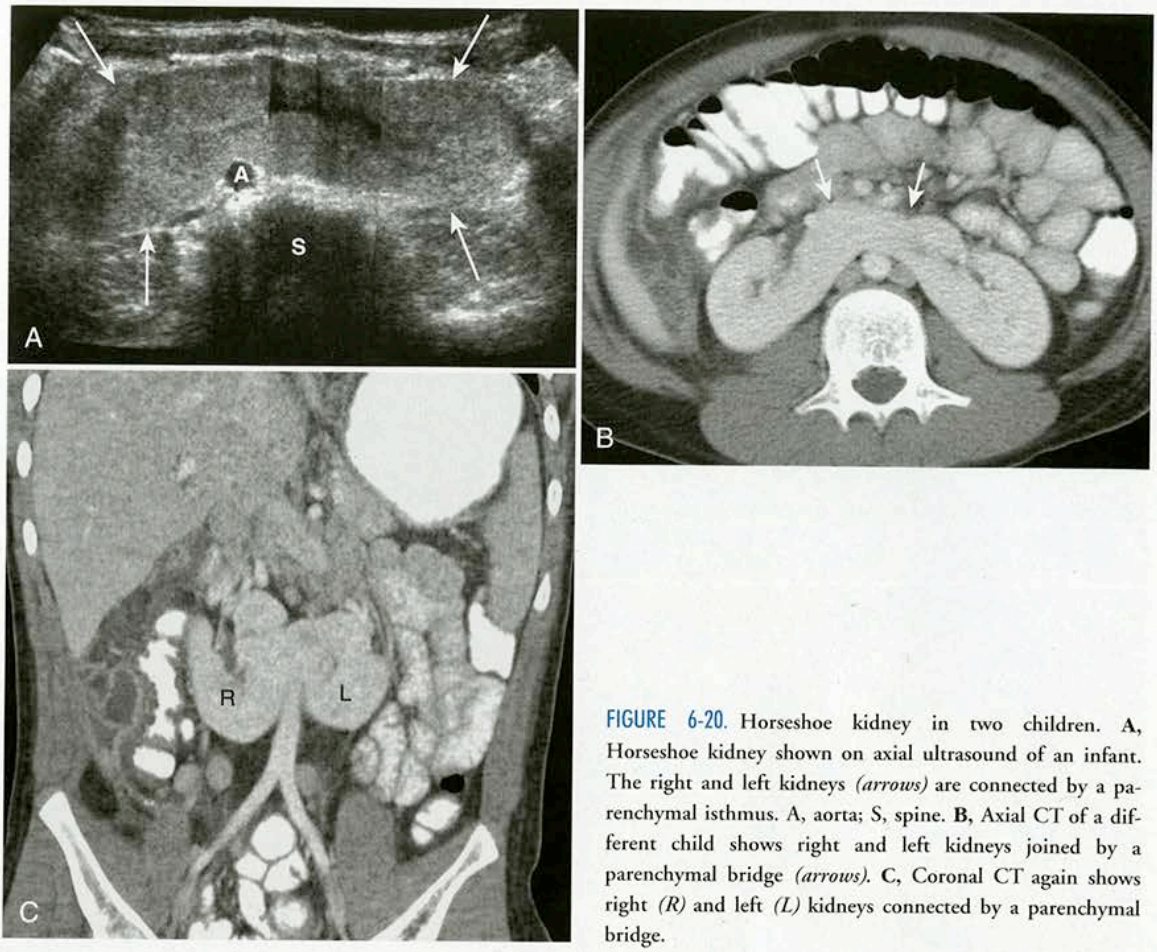

FIGURE 6-20. Horseshoe kidney in two children. **A,** Horseshoe kidney shown on axial ultrasound of an infant. The right and left kidneys *(arrows)* are connected by a parenchymal isthmus. A, aorta; S, spine. **B,** Axial CT of a different child shows right and left kidneys joined by a parenchymal bridge *(arrows).* **C,** Coronal CT again shows right *(R)* and left *(L)* kidneys connected by a parenchymal bridge.

(see Fig. 6-22). The bladder is trabeculated. Vesicoureteral reflux is present in approximately 50% of patients with posterior urethral valves.

Anything that relieves the increased pressure within the urinary system of patients with posterior urethral valves protects the patients from developing renal failure and is associated with a better prognosis. Such entities include unilateral vesicoureteral reflux (with protection of the kidney contralateral to the reflux; see Fig. 6-23), large bladder or calyceal diverticuli, or development of intrauterine ascites. It is the potential of posterior urethral valves that makes obtaining an image of the urethra during voiding a vital part of every VCUG performed on boys.

Urachal Abnormalities

The urachus is an embryologic structure that communicates between the apex of the bladder and the umbilicus. Normally, it closes by birth.

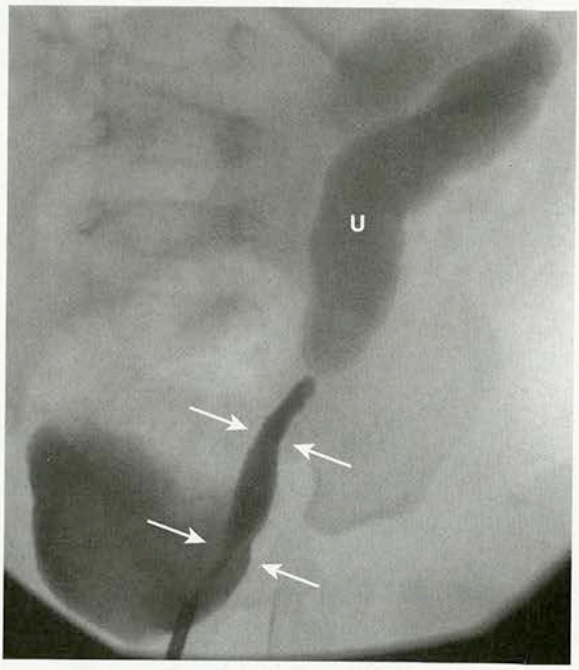

FIGURE 6-21. Primary megaureter. Retrograde contrast injection of ureter shows narrowed distal ureter *(arrows)* with dilatation of the more proximal ureter *(U),* secondary to relative obstruction.

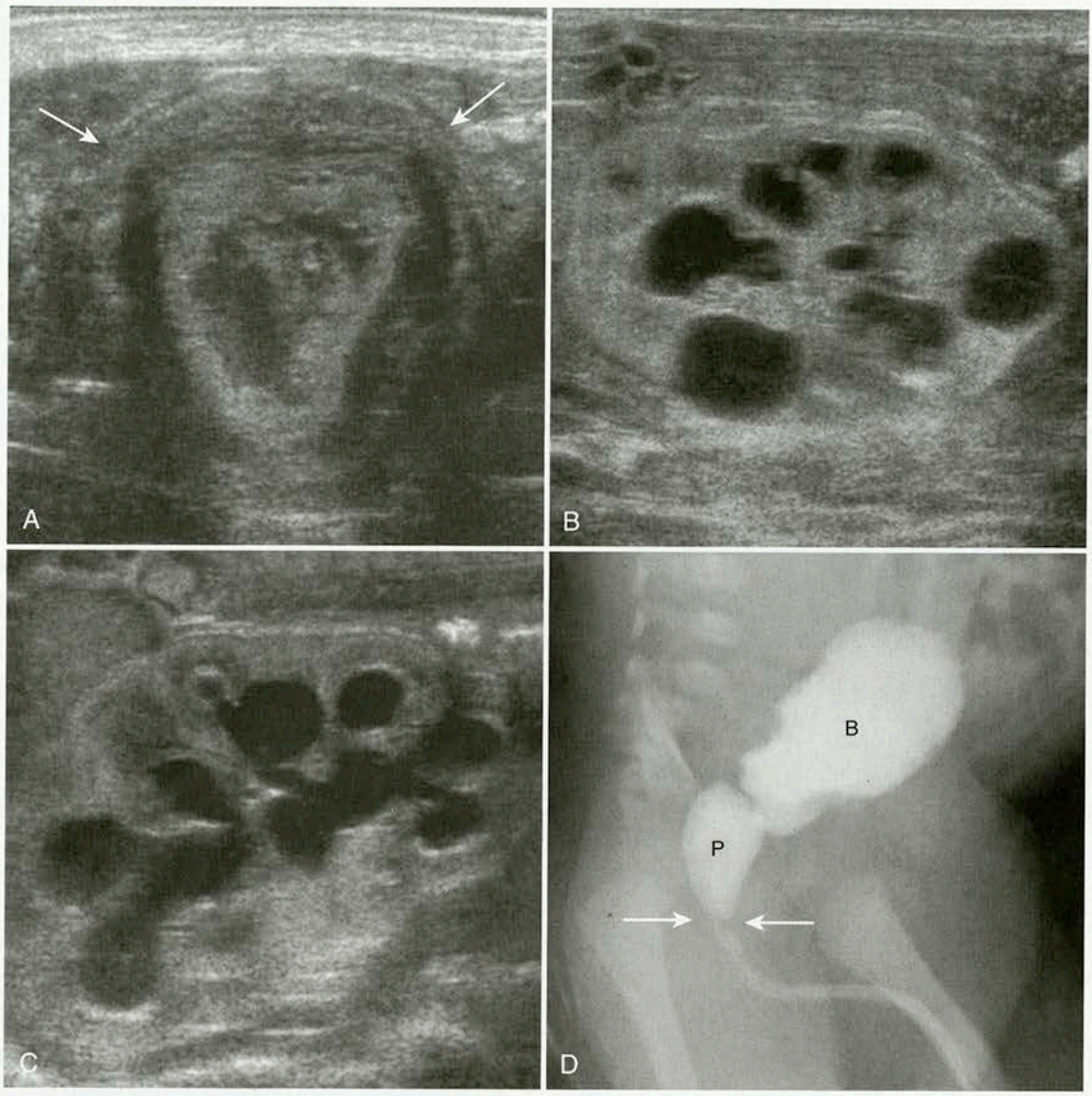

FIGURE 6-22. Posterior urethral valves in a newborn with renal failure. **A,** Axial ultrasound shows markedly thick-walled bladder *(arrows).* The bladder is empty. **B,** Longitudinal ultrasound of the left kidney shows hydronephrosis and echogenic renal parenchyma. **C,** Longitudinal ultrasound of the right kidney shows hydronephrosis and echogenic renal parenchyma. **D,** VCUG shows trabeculated, thick-walled bladder *(B),* dilatated posterior urethra *(P),* and visible posterior urethral valve *(arrows).*

If any portion of this embryologic structure remains patent, a urachal abnormality results. The type of the urachal anomaly present is determined by which portion of the urachus remains patent (Figs. 6-24, 6-25A-C). If the urachus remains patent in its entirety from the umbilicus to the bladder, it is a patent urachus (see Fig. 6-25). A neonate with a patent urachus will have urine draining from the umbilicus. Patent urachus can be demonstrated by VCUG, fistula tract injection, or ultrasound.

If the urachus remains patent only at the bladder end of the urachus, a urachal diverticulum is present. On ultrasound or VCUG, a diverticulum of variable size is demonstrated arising from the anterosuperior aspect of the dome on the bladder (see Fig. 6-25). Ultrasound may also demonstrate a fibrous tract extending from the diverticulum to the umbilicus.

If the urachus remains patent only at the umbilical end, a urachal sinus is present. If the urachus remains patent only at its midportion and is closed at both its umbilical and its bladder ends, a urachal cyst is present. Urachal cysts may present as palpable masses but more commonly present with inflammatory changes after becoming infected. Ultrasound or CT will show a cystic

mass anterior and superior to the bladder dome in the midline (see Fig. 6-25). Urachal carcinoma is rare in adults and extraordinarily rare in children.

Prune Belly Syndrome

Prune belly syndrome, or Eagle-Barrett syndrome, is the name given to the rare condition in which there is a triad of hypoplasia of the abdominal muscles, cryptorchidism, and abnormalities of the urinary tract system. Potential urinary tract abnormalities include severe bilateral hydronephrosis, a trabeculated and hypertrophied bladder, urachal diverticulum, and hydroureter. Radiographic manifestations include bulging flanks secondary to abdominal wall hypoplasia and the previously described renal manifestations (Fig. 6-26A, B). There are multiple associated congenital anomalies. Even more rarely, the syndrome can be incomplete (pseudo prune belly syndrome) in girls, who obviously cannot have cryptorchidism, and it can occur unilaterally.

Hydrometrocolpos

Genital outflow tract obstructions may lead to hydrometrocolpos or hematometrocolpos. *Hydrometrocolpos* is the term given to a rare condition in which the vagina and uterus dilate when fluid accumulates in the reproductive tract; this occurs in response to hormonal stimulation, so it occurs during infancy, secondary to maternal hormones, or during puberty. Hematometrocolpos is the accumulation of blood in a dilatated vagina and uterus that occurs after menarche in patients with a genital outflow tract obstruction. In both hydrometrocolpos and hematometrocolpos, a fixed midline mass may be palpable; the mass can become large enough to cause ureteral obstruction and result in hydronephrosis. Radiography or ultrasound can demonstrate the midline abdominal mass. On ultrasound, the mass appears tubular or elliptical and at the midline. In hematometrocolpos there is heterogeneous echogenicity secondary to the underlying hemorrhage (Fig. 6-27A, B). Because the vagina is more elastic, it becomes markedly dilatated and composes the bulk of the mass. The uterus may also be dilatated but cannot expand to the degree that the vagina can. Often the uterus can be identified as a small C-shaped cavity arising from the anterosuperior aspect of the distended vagina on ultrasound (see Fig. 6-27). Ultrasound also can reveal the degree of obstructive hydronephrosis. In problematic cases, MRI can be helpful in confirming the cause and the anatomy of the lesion (see Fig. 6-27).

Renal Cystic Disease

In children, renal cysts can occur secondary to polycystic kidney disease; can be associated with a variety of syndromes; can occur secondary to cystic neoplasms; or can be related to other cystic processes such as multicystic dysplastic kidney (Table 6-1). The categorization of and nomenclature for renal cystic disease in children can sometimes be confusing. In addition, it is important to note that although much less common than in adults, solitary simple renal cysts are not uncommonly identified in children. When such unilocular, solitary cysts are encountered during the workup for a urinary tract infection or hematuria, they are usually of no clinical significance and do not necessarily suggest an underlying developing polycystic kidney disease. As in adults, the ultrasound criteria for diagnosing a simple renal cyst include an anechoic, well-defined, round lesion; an imperceptible wall; and increased through-transmission. No central echoes or vascular flow is present within the lesion or within its walls.

Autosomal Recessive Polycystic Kidney Disease

Autosomal recessive polycystic kidney disease, also known as infantile polycystic kidney disease, encompasses a range of recessive diseases that are associated with varying amounts of cystic disease in the kidneys as well as with hepatic fibrosis. It is a very rare condition. When the renal findings (severe renal tubular ectasia) predominate, the disease most commonly presents on in utero imaging or during infancy and is termed infantile polycystic kidney disease. When the liver disease (severe fibrosis) predominates and there is minimal renal disease, the disease usually presents later in childhood and is referred to as juvenile polycystic kidney disease. In the infantile form, the kidneys are markedly enlarged and replaced by numerous small, 1- to 2-mm cysts throughout the cortex and medulla. On ultrasound, the kidneys are grossly enlarged and demonstrate

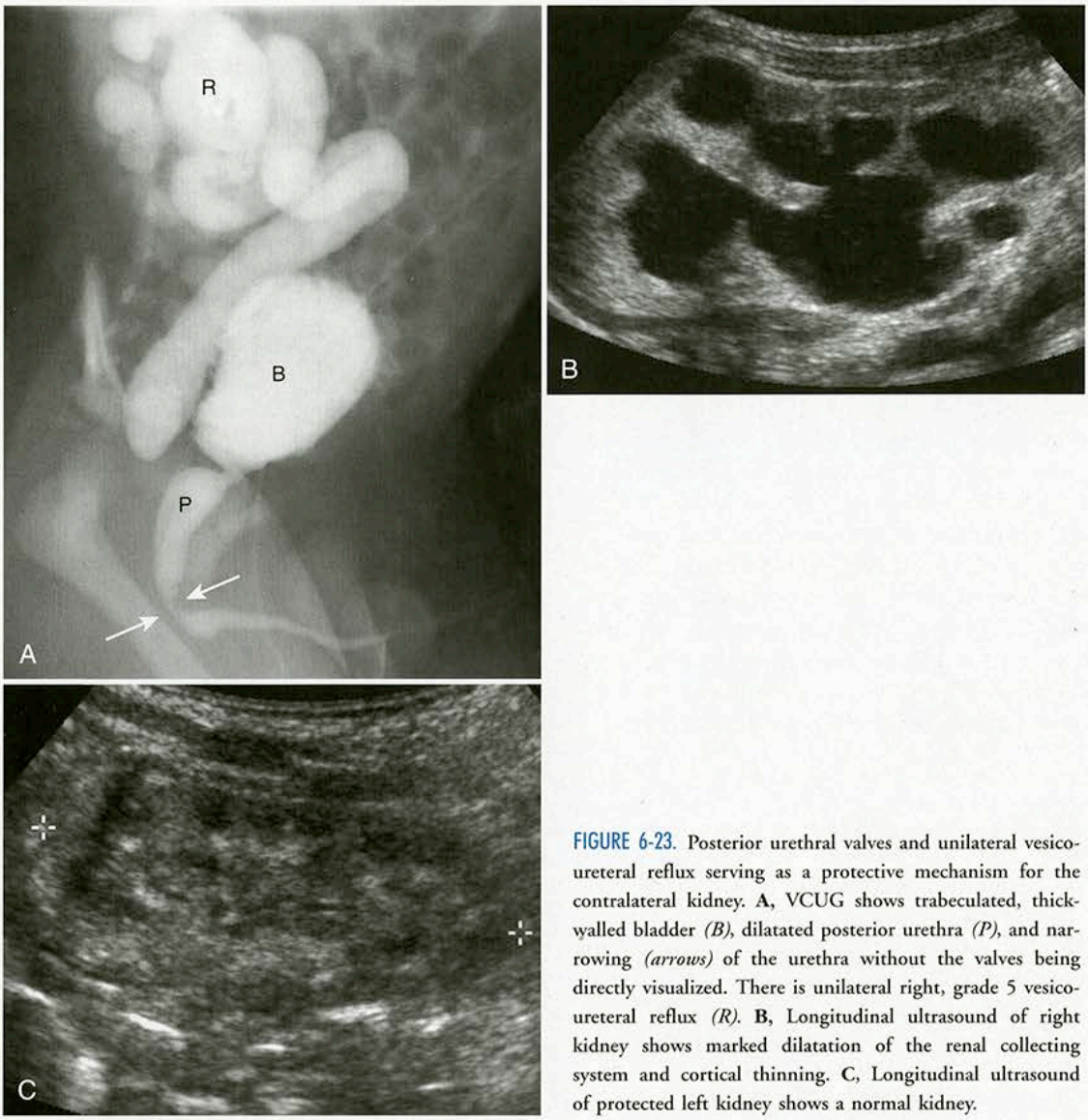

FIGURE 6-23. Posterior urethral valves and unilateral vesicoureteral reflux serving as a protective mechanism for the contralateral kidney. **A,** VCUG shows trabeculated, thick-walled bladder *(B)*, dilatated posterior urethra *(P)*, and narrowing *(arrows)* of the urethra without the valves being directly visualized. There is unilateral right, grade 5 vesicoureteral reflux *(R)*. **B,** Longitudinal ultrasound of right kidney shows marked dilatation of the renal collecting system and cortical thinning. **C,** Longitudinal ultrasound of protected left kidney shows a normal kidney.

diffuse increased echogenicity (Fig. 6-28A, B). Discrete cystic structures are sometimes not identified because of the small size of the cysts. In the juvenile form, patients usually present with hepatosplenomegaly and portal hypertension. The kidneys may demonstrate enlargement and cysts of varying sizes but may also appear normal. The liver usually shows increased echogenicity related to the diffuse hepatic fibrosis.

Autosomal Dominant Polycystic Kidney Disease

Autosomal dominant polycystic kidney disease, also known as adult polycystic kidney disease, is a dominantly inherited disease with variable penetrance. It is relatively common. Usually, the diagnosis is first encountered in early adulthood, when the patient presents with hypertension, hematuria, or renal failure. However, the cysts can be encountered during childhood. Some patients even present during the neonatal period. During childhood several cysts of varying sizes may be identified in both the cortex and medulla. The intervening renal parenchyma appears normal. The cysts gradually progress in size and number with time, and the normal renal parenchyma can be compressed and destroyed. Cysts may also be found in other organs, most commonly in the liver or pancreas. There is an association between the disease and the presence of intracranial berry aneurysms (10% of cases).

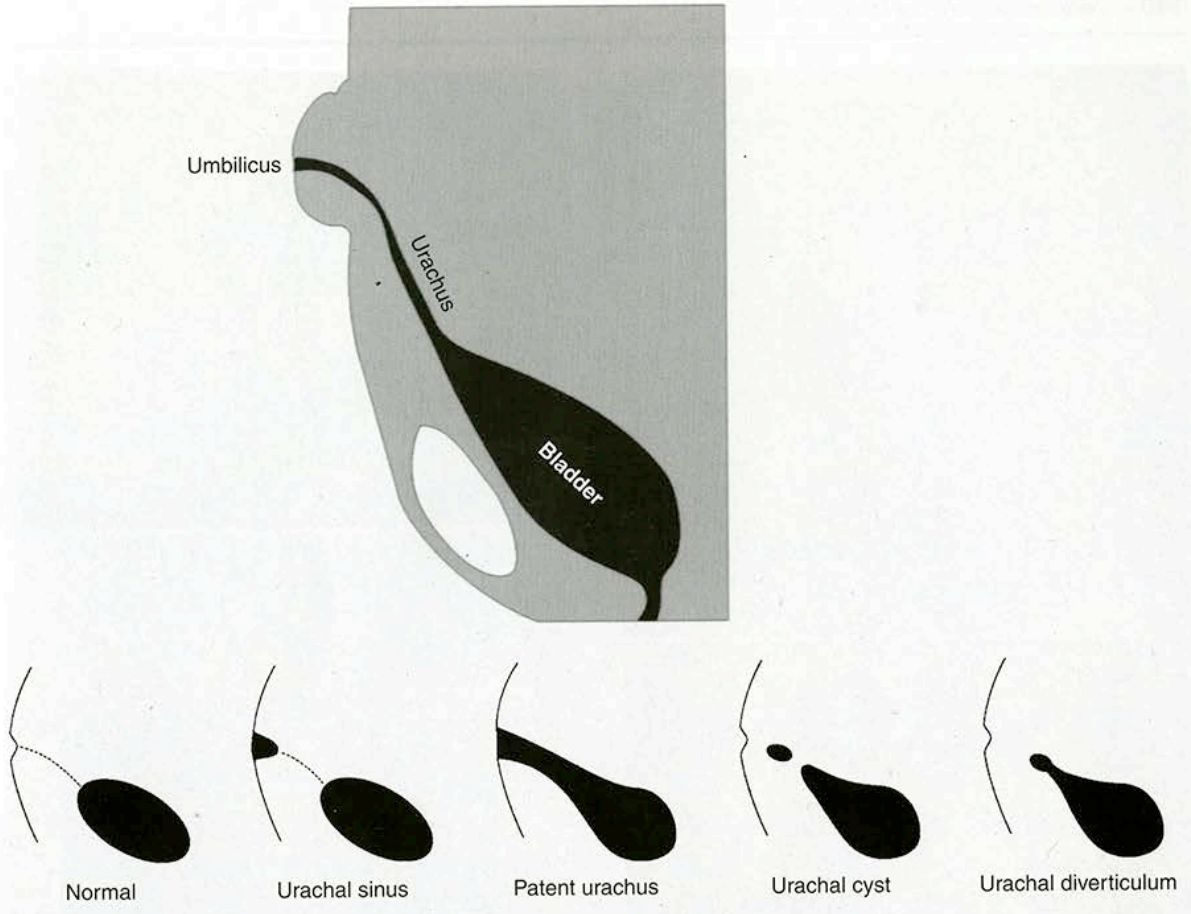

FIGURE 6-24. Urachal abnormalities. The superior image demonstrates the urachus as a patent connection between the umbilicus and bladder during fetal life. The inferior row of images demonstrates the potential urachal anomalies that occur when a portion or all of the urachus remains patent after birth. The type of urachal abnormality present depends upon which portion of the urachus remains patent.

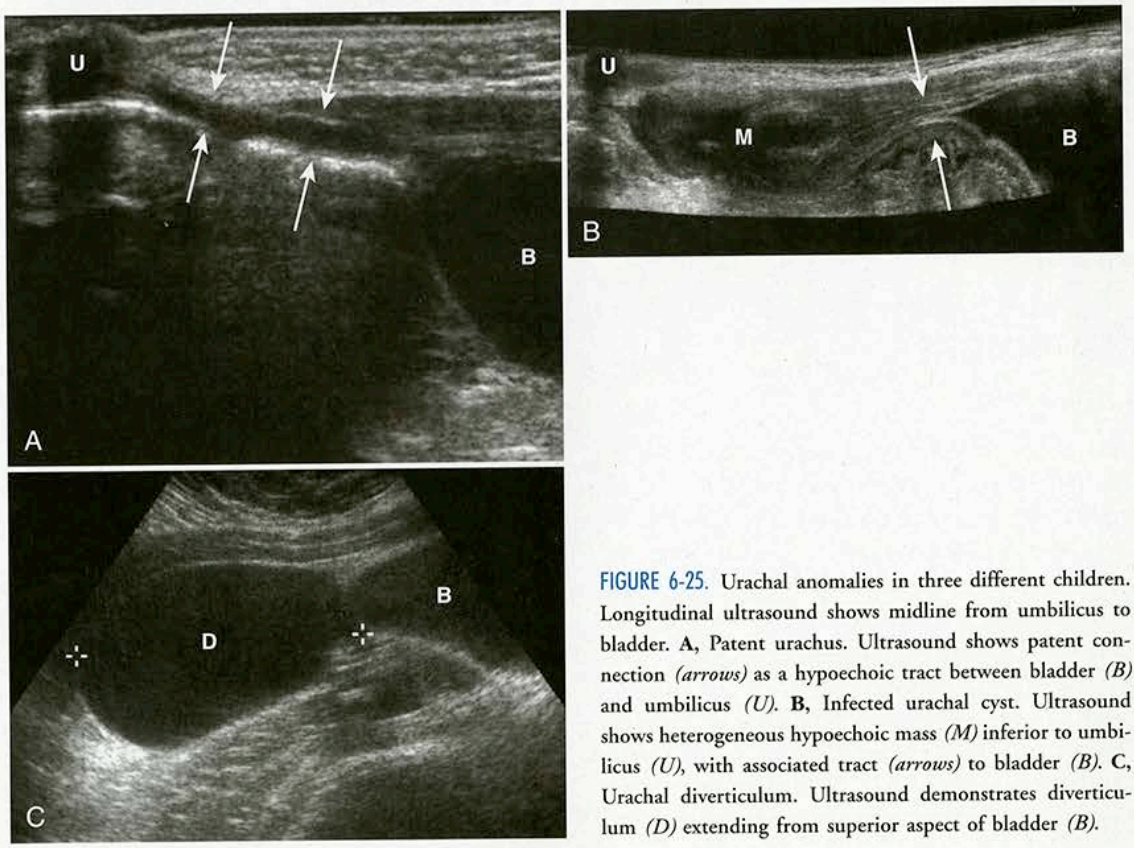

FIGURE 6-25. Urachal anomalies in three different children. Longitudinal ultrasound shows midline from umbilicus to bladder. **A,** Patent urachus. Ultrasound shows patent connection *(arrows)* as a hypoechoic tract between bladder *(B)* and umbilicus *(U)*. **B,** Infected urachal cyst. Ultrasound shows heterogeneous hypoechoic mass *(M)* inferior to umbilicus *(U)*, with associated tract *(arrows)* to bladder *(B)*. **C,** Urachal diverticulum. Ultrasound demonstrates diverticulum *(D)* extending from superior aspect of bladder *(B)*.

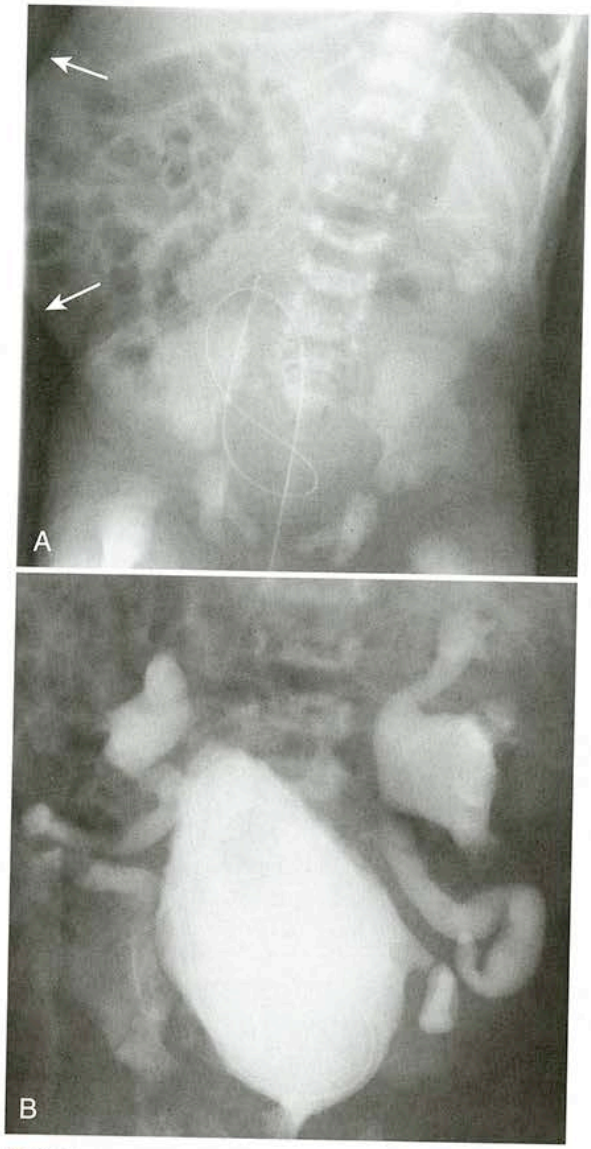

FIGURE 6-26. Prune belly syndrome. **A,** Radiograph shows bulging flanks *(arrows).* **B,** VCUG shows bilateral grade 5 VUR and trabeculated bladder.

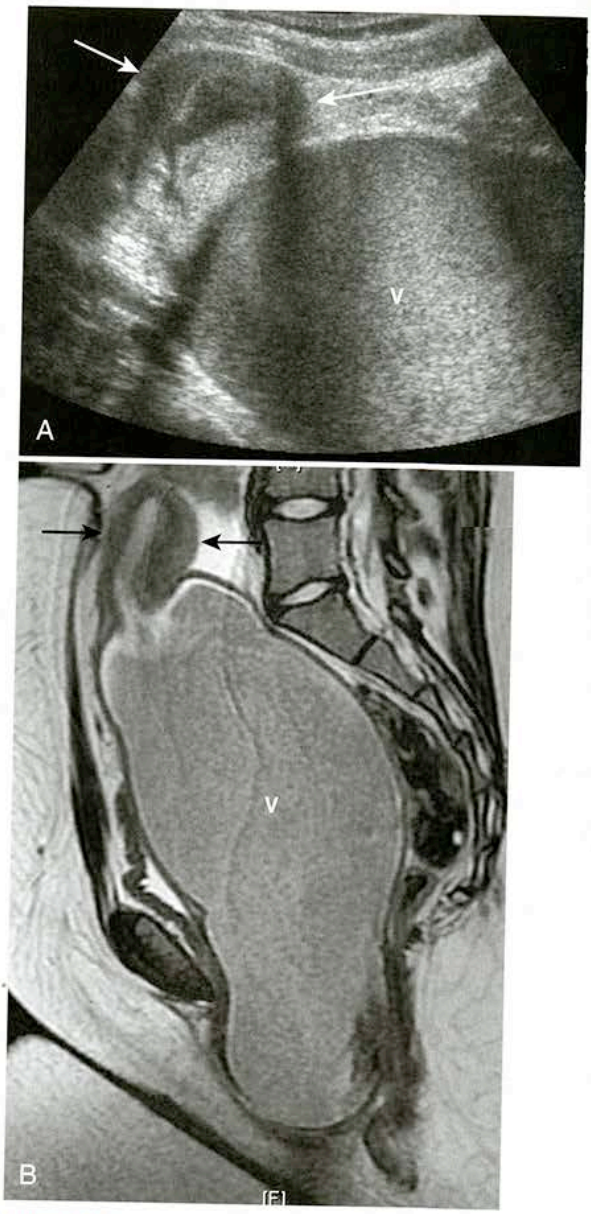

FIGURE 6-27. Hematometrocolpos shown in two different girls. **A,** Longitudinal midline ultrasound shows elliptical echogenic mass *(V),* which represents the vaginal cavity markedly distended with blood products. The uterus *(arrows)* extends from the superior aspect of the mass. The uterine cavity is slightly dilatated but not nearly as much as the vaginal cavity. **B,** Sagittal T1-weighted MRI of a different girl shows massively dilatated vaginal cavity *(V).* The uterus *(arrows)* extends from the superior aspect of the mass. The uterine cavity is slightly dilatated but not nearly as much as the vaginal cavity.

RENAL TUMORS

Wilms Tumor

Wilms tumor is the most common renal malignancy in children. It accounts for approximately 8% of all childhood malignant tumors. Also referred to as nephroblastoma, Wilms tumor is a malignant embryonal neoplasm. Its peak incidence occurs at approximately 3 years of age, with about 80% of cases detected between 1 and 5 years of age. Wilms tumor presents most commonly as an asymptomatic abdominal mass but may present with abdominal pain, particularly when there is intratumoral hemorrhage (Fig. 6-29A-C). Although most cases of Wilms tumor occur in otherwise normal children, there is an association between the development of Wilms tumor and overgrowth disorders (congenital hemihypertrophy, Beckwith-Wiedemann syndrome), sporadic aniridia, and other malformations. Wilms tumor can be bilateral in approximately 5% of cases. Invasion of the renal vein and extension into the renal vein into the inferior

TABLE 6-1. **Renal Cyst Disease in Children**

Solitary simple cyst
Autosomal recessive polycystic renal disease
Autosomal dominant polycystic renal disease
Multicystic dysplastic kidney
Syndromes
Tuberous sclerosis
von Hippel-Lindau
Meckel-Gruber
Cystic neoplasms
Wilms tumor
Multilocular cystic nephroma
Calyceal diverticulum

vena cava occurs commonly in Wilms tumor. Lung metastatic disease occurs in as many as 20% of cases.

On ultrasound, Wilms tumors typically appear as large, well-defined masses arising from the kidney (see Fig. 6-29). The masses are typically of increased echogenicity and may show heterogeneity related to areas of intratumoral hemorrhage, necrosis, or calcification. Doppler ultrasound is excellent in detecting extension of the tumor into the renal vein or inferior vena cava. It is especially important to document extension of the tumor thrombus into the right atrium because in such cases cardiothoracic surgery usually also becomes involved.

Confirmation of the lesion and evaluation of the anatomic extent of disease is usually performed using CT or MRI (Fig. 6-30A, B; and see Fig. 6-29). When evaluating a suspected Wilms tumor with either modality, it is important to document the following features: lymph node involvement, liver and lung metastases, involvement of the contralateral kidney by a synchronous Wilms tumor, the anatomic distribution of the intrarenal tumor, involvement of the renal vein or inferior vena cava, and the path of the ureters in relation to the mass. Identification of the ureter as anterior or posterior to the mass is important so that the ureters are not inadvertently injured when the mass is removed.

One of the most important issues when evaluating a mass in the region of the suprarenal fossa is determining whether the mass arises from the kidney and is therefore most likely a Wilms tumor or whether it arises from the suprarenal region and is a neuroblastoma. Differential features between these two lesions are described in Table 6-2. In the case of a Wilms tumor, the mass usually

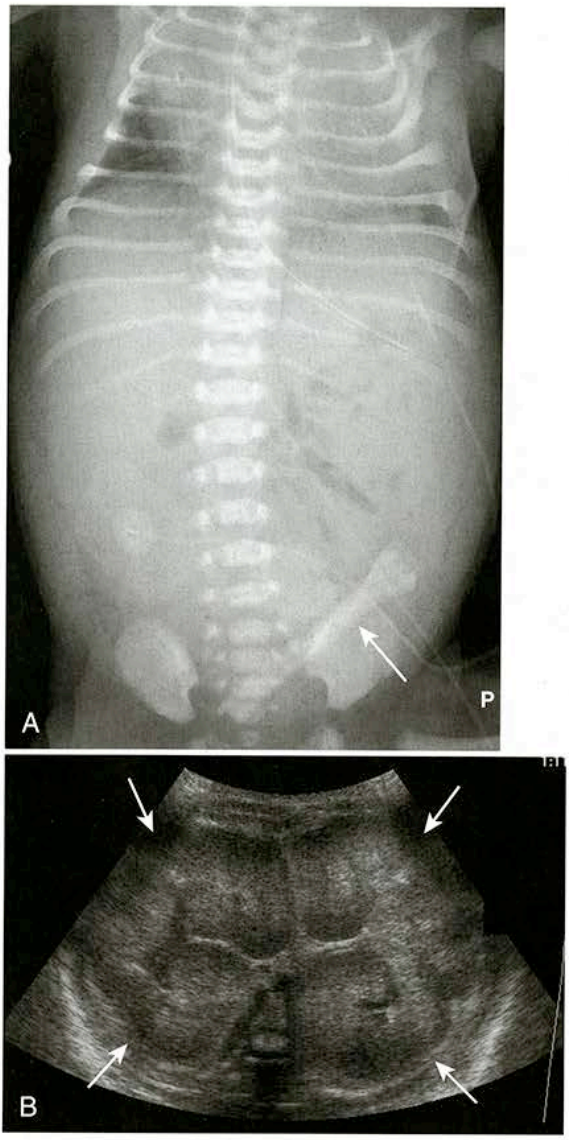

FIGURE 6-28. **Recessive polycystic kidney disease in an infant. A,** Radiography shows prominence of soft tissue in expected region of kidneys bilaterally. Incidentally, note the shadow caused by the umbilical clamp *(arrow)*, a common overlying artifact seen on radiographs of newborn infants. **B,** Axial ultrasound shows massive enlargement of bilateral kidneys *(arrows)*, which fill the majority of the abdominal cavity. The kidneys are of diffusely increased echogenicity, and no discrete cysts are identified.

appears as a well-defined, large, round mass on CT and MRI. The mass tends to grow in a ball, displacing blood vessels rather than engulfing them, as does neuroblastoma. As Wilms tumor arises in the kidney, the renal parenchyma often surrounds a portion of the mass, resulting in the "claw sign." When the mass crosses the midline, the lesion usually passes anterior to the aorta, as compared to neuroblastoma, which can surround the aorta posteriorly and raise it anteriorly, away

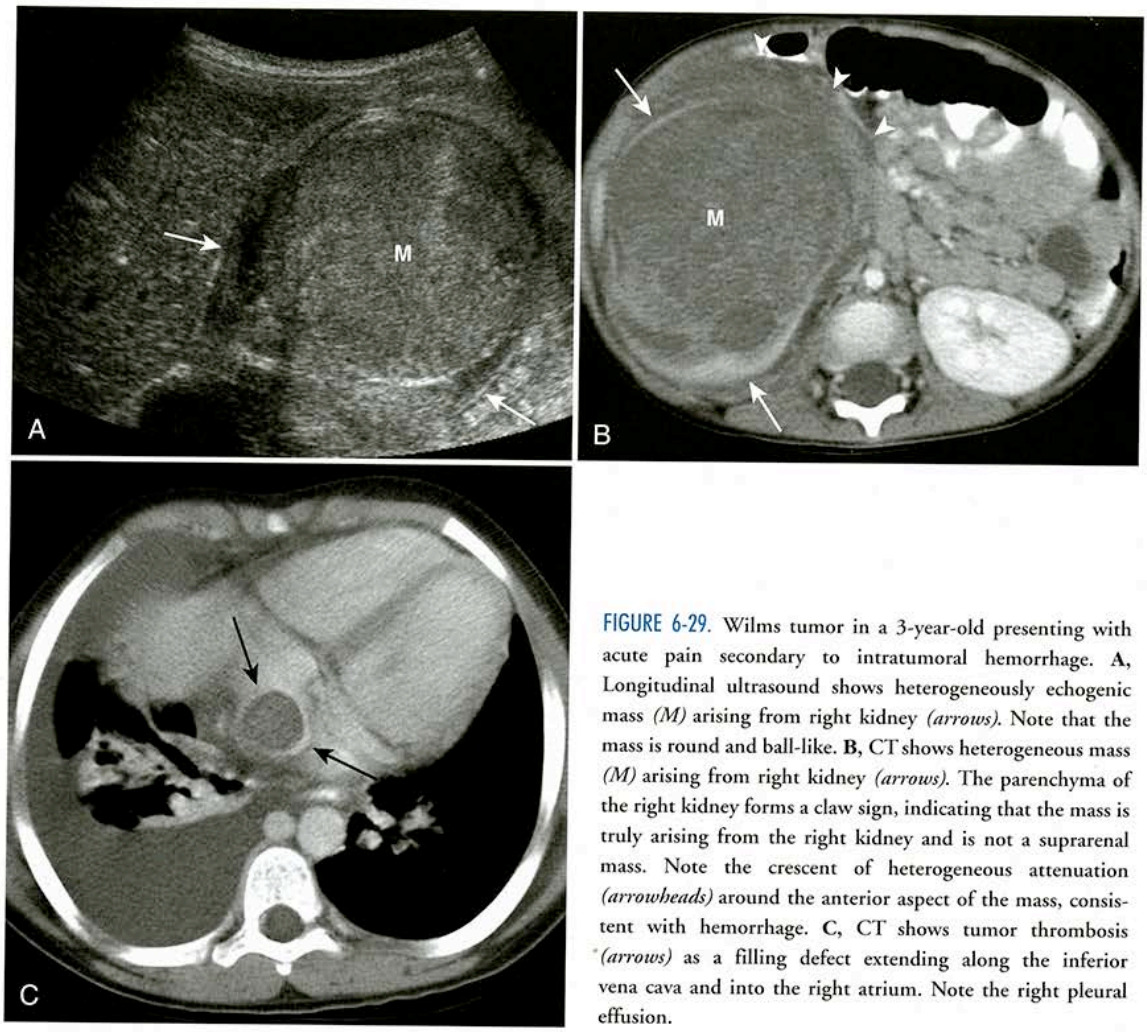

FIGURE 6-29. Wilms tumor in a 3-year-old presenting with acute pain secondary to intratumoral hemorrhage. **A,** Longitudinal ultrasound shows heterogeneously echogenic mass *(M)* arising from right kidney *(arrows)*. Note that the mass is round and ball-like. **B,** CT shows heterogeneous mass *(M)* arising from right kidney *(arrows)*. The parenchyma of the right kidney forms a claw sign, indicating that the mass is truly arising from the right kidney and is not a suprarenal mass. Note the crescent of heterogeneous attenuation *(arrowheads)* around the anterior aspect of the mass, consistent with hemorrhage. **C,** CT shows tumor thrombosis *(arrows)* as a filling defect extending along the inferior vena cava and into the right atrium. Note the right pleural effusion.

from the spine. Wilms tumors commonly appear to be solid, but larger lesions may have areas of heterogeneity or cystic components due to previous hemorrhage or necrosis.

Nephroblastomatosis

Nephroblastomatosis is a rare entity that is related to the persistence of nephrogenic rests within the renal parenchyma. These nephrogenic rests are precursors of Wilms tumors. Most patients with nephroblastomatosis are monitored by ultrasound, MRI, or CT for the development of Wilms tumors. On imaging, nephrogenic rests appear as plaquelike peripheral renal lesions and may be confluent (Fig. 6-31). The development of a Wilms tumor is suggested when a lesion appearing spherical demonstrates an increase in size compared to previous studies or demonstrates progressively increasing inhomogeneous enhancement as compared to the more nonenhancing nephrogenic rests. Typically, cases of Wilms tumor associated with syndromes are the ones that develop from nephroblastomatosis.

Multilocular Cystic Nephroma

Multilocular cystic nephroma is a rare type of cystic mass that contains multiple septa. The lesions have an unusual bimodal distribution in that they affect primarily young boys (3 months to 2 years) and adult women (during the fifth to sixth decades). Typically, the lesions present as a painless abdominal mass. By definition, the lesions do not contain malignant cells but can be difficult to distinguish from a well-differentiated Wilms tumor on imaging. On ultrasound, CT, and MRI, the lesions appear as well-circumscribed, multiseptated masses (Fig. 6-32A-D). Because the lesions cannot be differentiated from malignancy at imaging, surgical resection is performed.

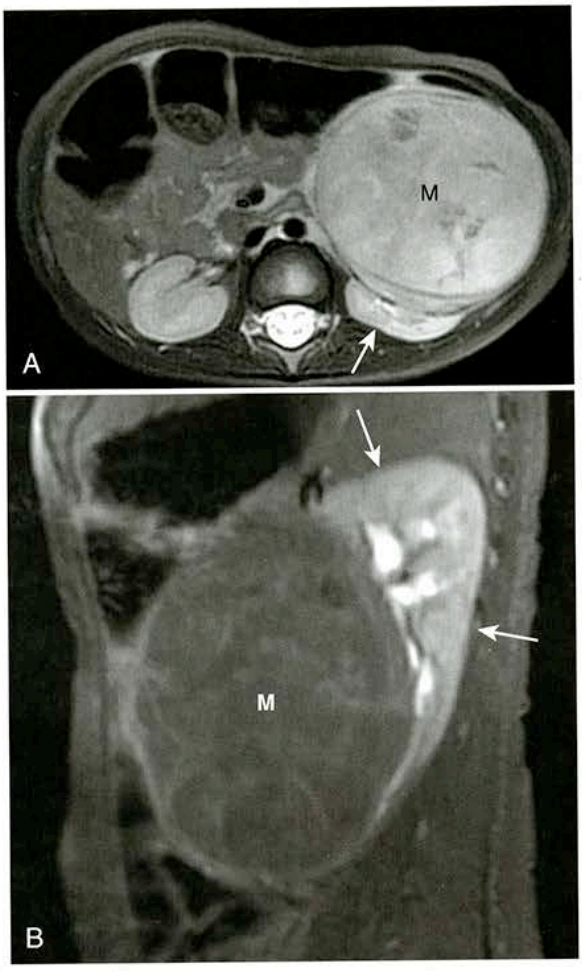

FIGURE 6-30. Wilms tumor on MRI. **A,** Axial T2-weighted image shows mass *(M)* arising from left kidney *(arrow).* The lesion is heterogeneous in signal and is round. **B,** Sagittal post-contrast image shows low signal mass *(M)* and enhancing surrounding renal parenchyma *(arrows).*

Mesoblastic Nephroma

Mesoblastic nephroma, or fetal renal hamartoma, is the most common renal mass in neonates. Typically, it is encountered prenatally or during the first few months of life; the mean age of diagnosis is approximately 3 months. Neonates most commonly present with a nontender, palpable abdominal mass. The lesion consists of benign spindle-type cells. Ultrasound demonstrates a mixed echogenic mass that is intrarenal in location and indistinguishable from a Wilms tumor. CT demonstrates a solid intrarenal mass with variable enhancement (Fig. 6-33A, B).

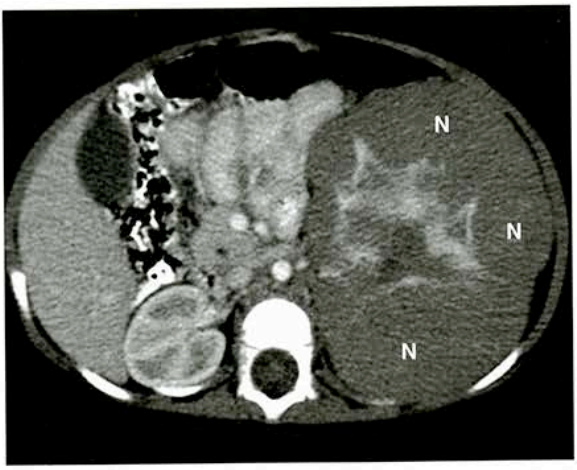

FIGURE 6-31. Nephroblastomatosis. CT shows peripheral plaquelike lesions *(N)* of low attenuation. The lesions circumferentially involve the left kidney and distort the central renal parenchyma. In this case, the right kidney is normal.

Other Renal Tumors

Other, less common causes of malignant renal lesions include renal cell carcinoma, renal lymphoma, clear cell carcinoma, and rhabdoid tumor. Renal cell carcinoma is the most common cause of renal malignancy in older children, although it is still much less common than in adults. Ultrasound and CT typically show a nonspecific solid renal mass. Calcification is more common with renal cell carcinoma (25%) than with Wilms tumor.

TABLE 6-2. **Differentiating Features Between Neuroblastoma and Wilms Tumor**

Feature	Neuroblastoma	Wilms Tumor
Age	Most common before age 2 years	Peak incidence at 3 years
Calcification	Calcifications common (85% on CT) and stippled	Calcifications uncommon (15% on CT) and often curvilinear or amorphous
Growth pattern	Surrounds and engulfs vessels	Grows like ball, displacing vessels
Relation to kidney	Inferiorly displaces and rotates kidney	Arises from kidney, claw sign
Lung metastasis	Uncommon	More common (20%)
Vascular invasion	Does not occur	Invasion of renal vein/inferior vena cava

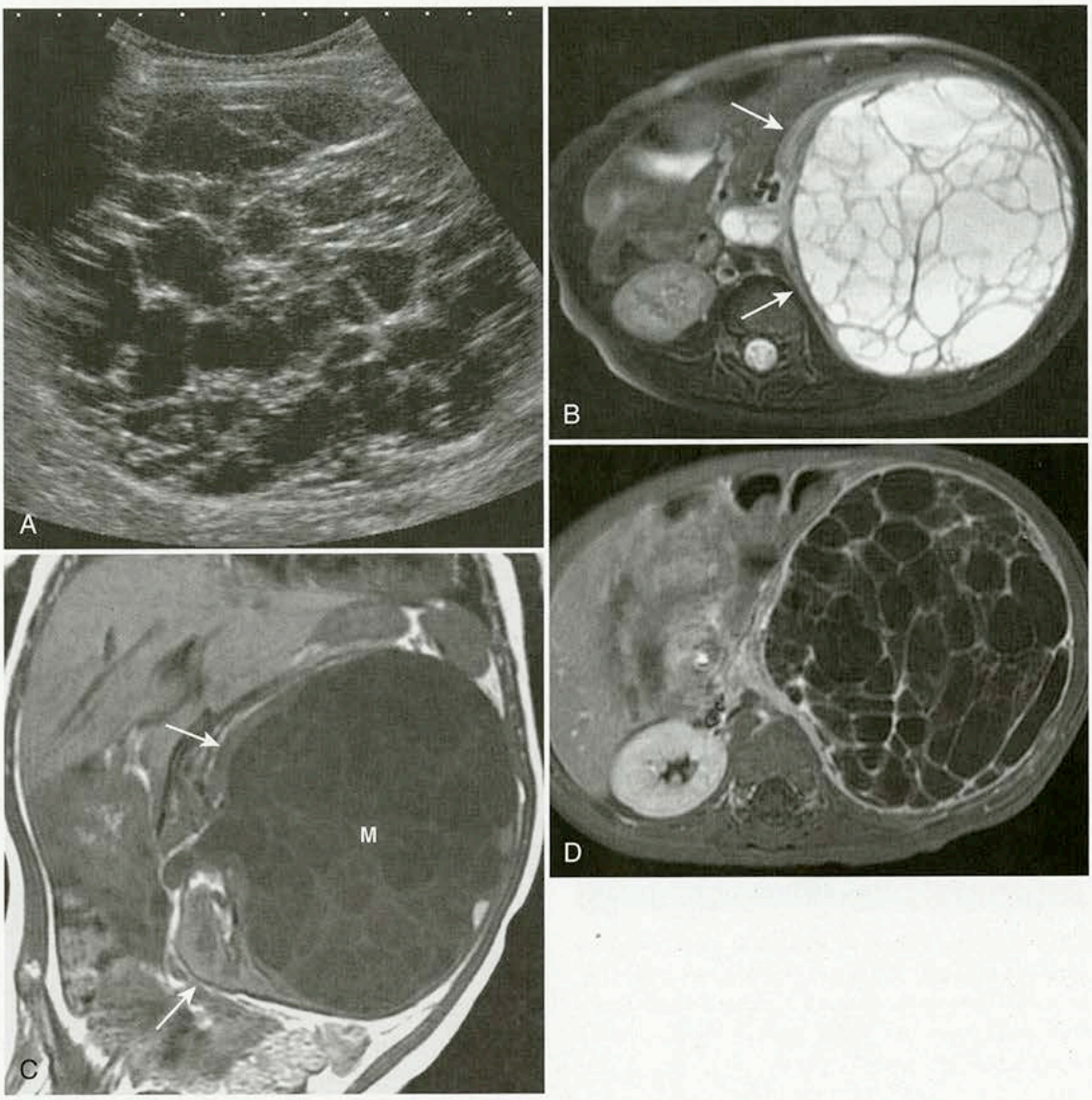

FIGURE 6-32. Multilocular cystic nephroma. **A,** Ultrasound shows a multiloculated cystic mass in the left kidney. **B,** T2-weighted, axial MR image shows multiseptated cystic mass. Note "claw sign" indicating origin of mass in left kidney *(arrows).* **C,** T1-weighted, coronal MRI shows low signal in cystic structures within mass *(M).* Again, note renal parenchyma *(arrows)* surrounding the medial aspect of the mass. **D,** Postcontrast, axial MR image shows only septal enhancement of cyst walls without solid components.

Angiomyolipoma

Patients with tuberous sclerosis are predisposed to developing angiomyolipomas. These lesions commonly demonstrate fatty components on imaging (Fig. 6-34A, B) and may spontaneously hemorrhage. Hemorrhage from angiomyolipomas is the leading cause of death in tuberous sclerosis patients. Angiomyolipomas bigger than 4 cm in diameter are particularly predisposed to contain dysplastic arteries and aneurysms that may hemorrhage; they are commonly treated by prophylactic embolization. The angiomyolipomas start as small echogenic foci within the kidneys during early childhood (Fig. 6-35) and grow into large infiltrative masses that enlarge the kidneys (see Fig. 6-34). Tuberous sclerosis is also associated with autosomal dominant polycystic kidney disease and renal cysts.

ADRENAL GLANDS

A number of pathologic processes can involve the adrenal glands in children. The most commonly encountered adrenal disorders are neuroblastoma and neonatal adrenal hemorrhage.

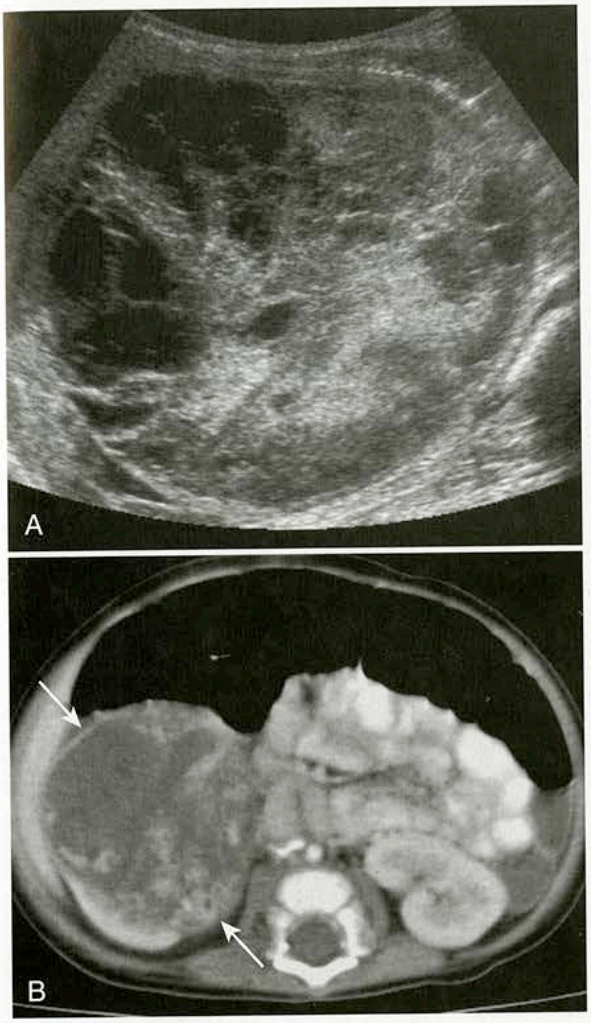

FIGURE 6-33. Mesoblastic nephroma in two neonates. **A,** Ultrasound shows a heterogeneous mass in the right kidney of a neonate. **B,** CT in another neonate shows a heterogeneously enhancing right renal mass *(arrows).*

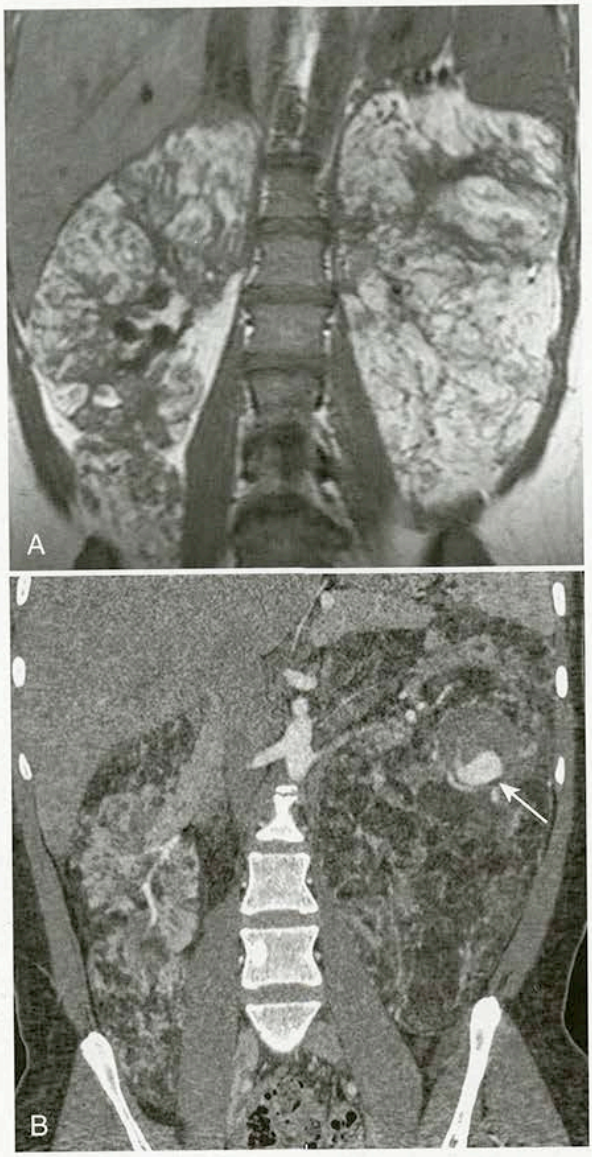

FIGURE 6-34. Advanced angiomyolipomas. **A,** T1-weighted coronal MR image shows diffuse fatty infiltration and enlargement of the bilateral kidneys. **B,** Coronal CT shows diffuse fatty infiltration and enlargement of the bilateral kidneys. There is contrast enhancement *(arrow)* within a partially thrombosed aneurysm in the left kidney.

Neuroblastoma

Neuroblastoma is a malignant tumor of primitive neural crest cells that most commonly arises in the adrenal gland but can occur anywhere along the sympathetic chain. It is differentiated from its more benign counterparts, ganglioneuroma and ganglioneuroblastoma, by the degree of cellular maturation. Neuroblastoma is an aggressive tumor with a tendency to invade adjacent tissues. The tumor metastasizes most commonly to liver and bone. It is the most common extracranial solid malignancy in children and the third most common malignancy of childhood, with only leukemia and primary brain tumors being more common. Approximately 90% to 95% of patients with neuroblastoma have elevated levels of catecholamines (vanillylmandelic acid) in their urine, a useful diagnostic tool.

Neuroblastoma is a very unusual tumor in that the prognosis and the patterns of distribution of disease depend strongly on age. In children who are less than 1 year of age, the disease tends to spread to liver and skin; they usually have a good prognosis. In those older than 1 year of age, the disease tends to spread to bone; they have a poorer prognosis. The staging (Evans) system for neuroblastoma is unique (Table 6-3). There is a special stage "IV s" that is given to children less than 1 year of age with

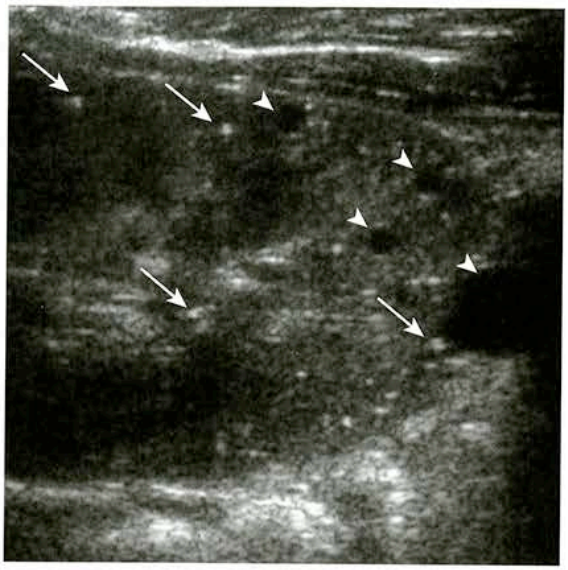

FIGURE 6-35. **Angiomyolipoma in a 5 year old with tuberous sclerosis. Ultrasound shows multiple punctuate echogenic foci in the kidney. The most prominent echogenic foci are denoted by *arrows*. There are also multiple small cysts *(arrowheads)*.**

metastatic disease that is confined to skin, liver, and bone marrow (Fig. 6-36A-D). Cortical bone involvement demonstrated by radiography or nuclear bone scintigraphy is not considered stage IV s. It is intriguing that patients with stage IV disease have very poor prognoses and commonly require therapy such as bone marrow transplantation, whereas patients with stage IV s disease have excellent prognoses and at many institutions are watched with imaging and

TABLE 6-3. **Evans Anatomic Staging for Neuroblastoma**

Stage	Definition	Prognosis (% survival)
I	Tumor confined to organ of origin	90
II	Tumor extension beyond organ of origin but not crossing midline	75
III	Tumor extension crossing midline	30
IV	Disseminated disease (skeleton or distant soft tissues, lymph nodes, and organs)	10
IV s	Age less than 1 year	Near 100
	Primary tumor with metastatic disease to skin, liver, or bone marrow	Often, no therapy

receive no therapy. Other factors associated with better prognoses are listed in Table 6-4.

Although neuroblastoma may be encountered initially as a mass on abdominal radiographs or ultrasound, confirmation of the diagnosis and definition of the exact extent of disease is obtained with either CT or MRI. Some investigators have advocated MRI over CT because of its superior ability to identify tumor extension into the neuroforamina. Neuroforaminal involvement is important to identify because, at many institutions, it will lead neurosurgery services to become involved in the surgical resection. In my experience, both CT and MRI are excellent in identifying neuroforaminal and spinal canal involvement.

On CT, neuroblastoma is detected with a sensitivity of nearly 100%. The tumors tend to appear lobulated and to grow in an invasive pattern, surrounding and engulfing, rather than displacing, vessels such as the celiac axis, superior mesenteric artery, and aorta (Fig. 6-37). The masses are often inhomogeneous secondary to hemorrhage, necrosis, and calcifications. Calcifications are seen by CT in as much as 85% of cases (see Fig. 6-37). On MRI, neuroblastoma, like most other malignancies, appears bright on T2-weighted images and can be heterogeneous in signal. Calcifications are less commonly seen on MRI. During the staging of neuroblastoma, most patients also undergo evaluation by metaiodobenzylguanidine (MIBG) and bone scintigraphy. The role of positron emission tomography (PET) and PET/CT is still being defined.

Other adrenal tumors that occur in childhood, but much less commonly than neuroblastoma, include pheochromocytoma and adrenal carcinoma.

Neonatal Adrenal Hemorrhage

Adrenal hemorrhage can occur in neonates secondary to birth trauma or stress. Like neuroblastoma, adrenal hemorrhage may present as an asymptomatic flank mass and may be seen on imaging as an adrenal mass. Surgical intervention is unnecessary in adrenal hemorrhage, so differentiation from neuroblastoma is important. Ultrasound is usually able to differentiate the two. Neuroblastoma typically appears as an echogenic mass with diffuse vascularity (color Doppler), whereas adrenal hemorrhage typically appears as an anechoic, avascular mass (Fig. 6-38). Performing serial ultrasounds over time (see Fig. 6-38) is an acceptable way of

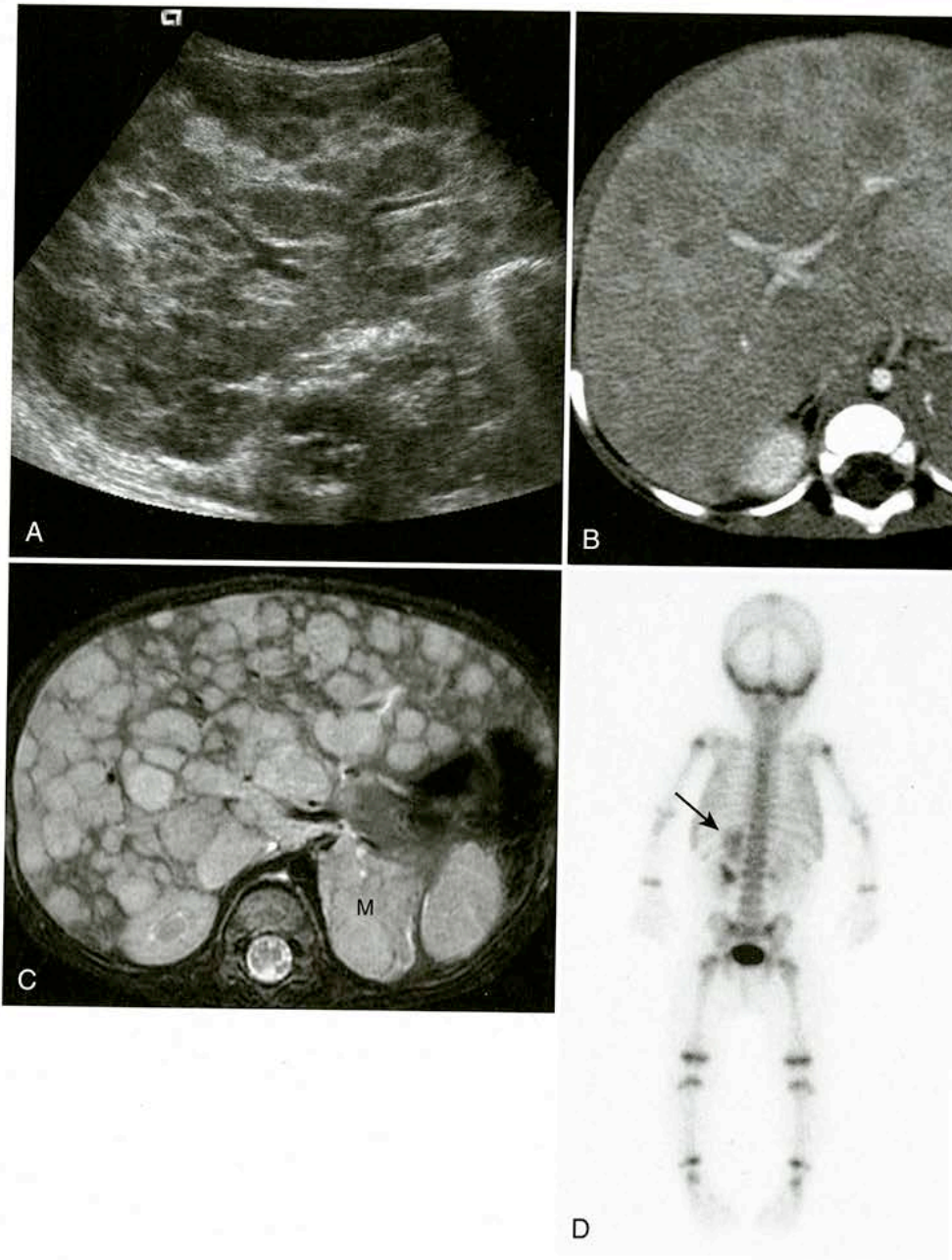

FIGURE 6-36. Stage IV s neuroblastoma in a 9-month-old boy with palpable fullness in abdomen. **A**, Ultrasound shows multiple heterogeneous hypoechoic masses throughout the liver parenchyma. **B**, CT shows left suprarenal mass *(M)*. There are multiple low-attenuation metastatic lesions in the liver. **C**, T2-weighted axial MRI shows multiple liver metastatic lesions more clearly and again demonstrates left adrenal mass *(M)*. **D**, MIBG study (oriented with left side of patient on left of image) shows increased uptake in left adrenal mass *(arrow)*. There is downward displacement of the left renal collecting system.

differentiating problematic cases because the prognosis for neonates with stage I neuroblastoma is excellent. With time, adrenal hemorrhages decrease in size. MRI can also be useful in differentiating adrenal hemorrhage (low T2-weighted signal, blood product signal) from neuroblastoma (high T2-weighted signal) in very problematic cases.

PELVIC RHABDOMYOSARCOMA

Rhabdomyosarcoma is a highly malignant tumor that can occur in numerous locations throughout the body. It is the most common malignant sarcoma of childhood and typically presents during the first 3 years of life. Its most common locations include the pelvis and genitourinary tract

TABLE 6-4. **Features Associated with Better Prognosis in Patients With Neuroblastoma**

Age of diagnosis less than 1 year
Histiologic grade
Decreased n-myc amplification
Stage IV s
Thoracic primary

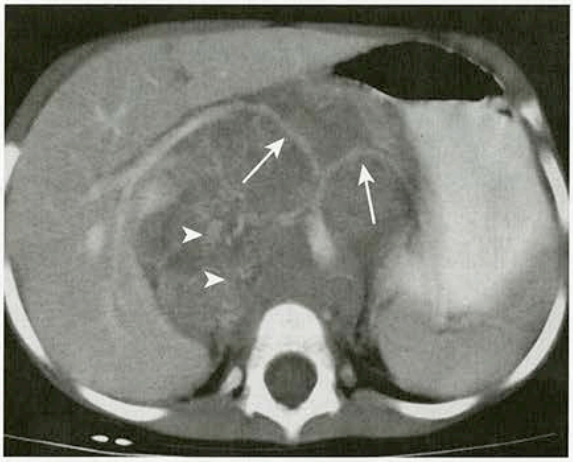

FIGURE 6-37. Neuroblastoma in a 2-year-old girl. CT shows heterogeneously enhancing retroperitoneal mass that surrounds and anteriorly displaces the abdominal aorta and engulfs and surrounds the branches *(arrows)* of the celiac artery. Note the heterogeneous calcifications *(arrowheads)*.

(39%) and the head and neck (39%). The most common locations within the genitourinary tract include the bladder, prostate (Fig. 6-39A, B), spermatic cord, paratesticular tissues, uterus, vagina, and perineum. It affects girls and boys equally. When the lesion involves the bladder, it typically appears as a multilobulated mass, likened to a bunch of grapes. Pelvic rhabdomyosarcoma may result in hydronephrosis.

SACROCOCCYGEAL TERATOMA

Sacrococcygeal teratomas typically present as large cystic or solid masses either on prenatal imaging or at birth. Less commonly, they present as buttock asymmetry or a presacral mass later in childhood. The majority are benign, but there is an increased risk for malignancy with delayed diagnosis. The masses can be primarily external (47%), internal within the pelvis (9%), or dumbbell-shaped, with both internal and external components (34%). On imaging, the lesions

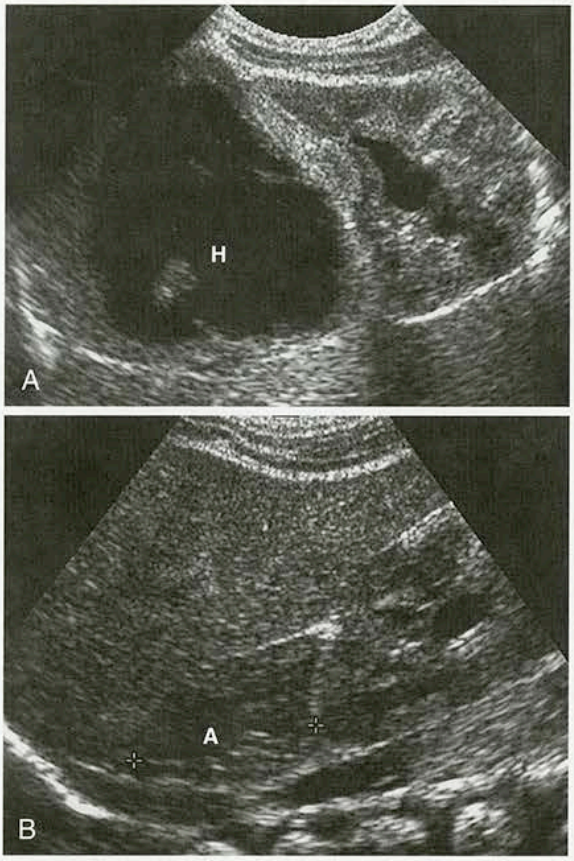

FIGURE 6-38. Adrenal hemorrhage in a 4-day-old neonate. **A,** Initial sonogram shows predominantly cystic-appearing, hypoechoic mass *(H)* in a suprarenal location. The kidney is displaced inferiorly. **B,** Follow-up ultrasound from approximately 1 month later shows marked interval decrease in the size of the adrenal gland *(A)*, a more adrenoform shape, and resolution of the cystic appearance, consistent with resolving hematoma.

appear heterogeneous, with variable cystic, solid, and fatty components (Fig. 6-40A-E).

SCROTUM

The commonly encountered imaging issues in the pediatric scrotum include testicular neoplasm, testicular microlithiasis, and the acutely painful scrotum. Of testicular neoplasms, 90% are germ cell in origin. Less than 10% of testicular tumors are metastatic from leukemia or lymphoma. Most primary testicular tumors present with a nontender, firm scrotal mass. Ultrasound confirms an intratesticular mass (Fig. 6-41). However, there are no ultrasound findings that suggest a specific histologic diagnosis. If a scrotal mass is extratesticular in location, the most likely diagnosis is embryonal rhabdomyosarcoma arising from the spermatic cord or epididymis.

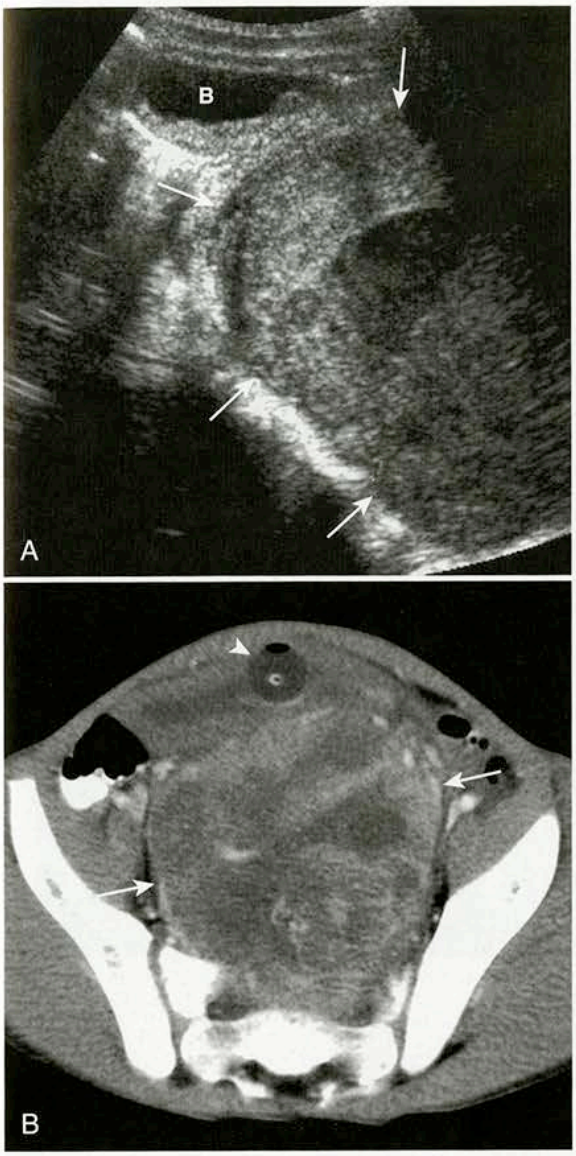

FIGURE 6-39. Rhabdomyosarcoma arising from the prostate in a boy. **A,** Longitudinal ultrasound shows large heterogeneous mass *(arrows)* arising from the pelvis and displacing the bladder *(B).* **B,** CT shows a large heterogeneous mass *(arrows)* arising from the pelvis and displacing the bladder anteriorly (Foley catheter balloon demarcated by *arrowhead*).

Testicular Microlithiasis

Testicular microlithiasis appears on ultrasound as multiple small echogenicities within the testes (Fig. 6-42). There is often no posterior acoustic shadowing because of the small size of the calcifications. The finding is typically seen incidentally when the scrotum is being imaged for other reasons. It was initially reported that the risk for development of testicular neoplasm was between 18% and 75% in patients with ultrasound-demonstrated testicular microlithiasis. This led to recommendations for serial screening ultrasounds in patients with testicular microlithiasis to exclude development of neoplasm. However, more recent reports have shown that testicular microlithiasis is much more common than initially suspected, occurring in about 6% of the male population between 17 and 35 years of age. These reports have also shown that the overwhelming majority of these patients will not develop malignancies. Some now advocate following such patients with physical examination rather than ultrasound.

The Acute Scrotum

Because of the possibility of testicular torsion, imaging of the acutely painful scrotum is an emergency. The major differential considerations in a child with acute scrotal pain include testicular torsion, epididymoorchitis, and torsion of the testicular appendage. Testicular hematoma is another less commonly encountered entity. The most common entities encountered in the setting of acute scrotal pain are actually epididymoorchitis and torsion of the testicular appendage. Although ultrasound examinations are performed to rule out testicular torsion, it is actually much less common than the other entities.

Testicular torsion occurs when the testis and cord twist within the serosal space and cause testicular ischemia. Prompt diagnosis and therapy are important because preservation of the testis is possible only in patients whose torsion is relieved within 6 to 10 hours. Color Doppler ultrasound has replaced testicular scintigraphy as the modality of choice in evaluating an acute scrotum. Color Doppler demonstrates absence of flow or asymmetrically decreased flow within the affected testis (Fig. 6-43A, B). Demonstration of flow within a normal testis is more difficult in children less than 2 years of age. Gray-scale ultrasound may demonstrate asymmetric enlargement and slightly decreased echogenicity of the affected testis (see Fig. 6-43). With progressive ischemia or infarction, hemorrhage and necrosis may cause increasing asymmetric heterogeneity (see Fig. 6-43). This is a late finding.

Epididymoorchitis usually occurs without an identifiable cause. In contrast to testicular torsion,

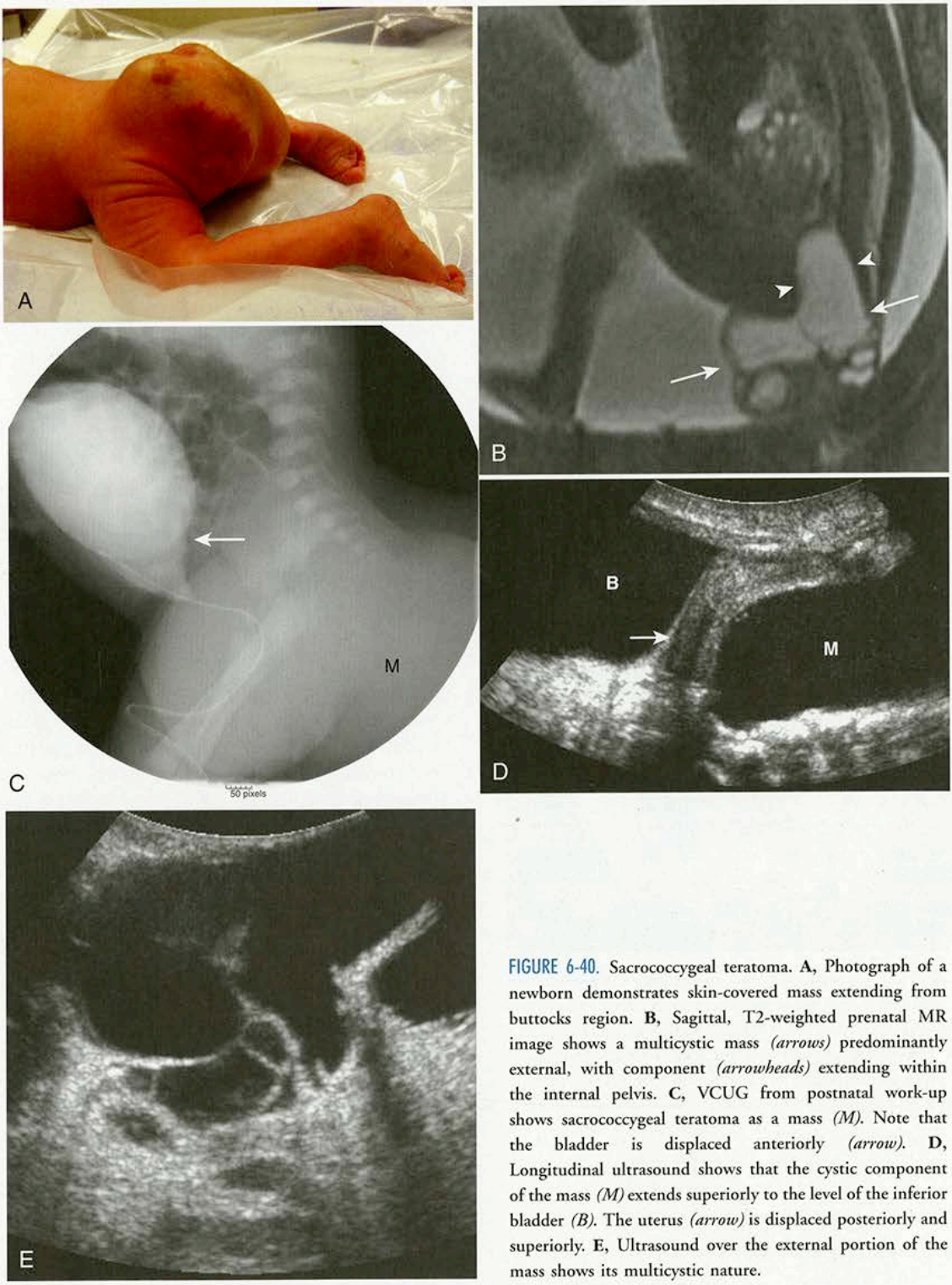

FIGURE 6-40. Sacrococcygeal teratoma. **A,** Photograph of a newborn demonstrates skin-covered mass extending from buttocks region. **B,** Sagittal, T2-weighted prenatal MR image shows a multicystic mass *(arrows)* predominantly external, with component *(arrowheads)* extending within the internal pelvis. **C,** VCUG from postnatal work-up shows sacrococcygeal teratoma as a mass *(M)*. Note that the bladder is displaced anteriorly *(arrow)*. **D,** Longitudinal ultrasound shows that the cystic component of the mass *(M)* extends superiorly to the level of the inferior bladder *(B)*. The uterus *(arrow)* is displaced posteriorly and superiorly. **E,** Ultrasound over the external portion of the mass shows its multicystic nature.

in epididymoorchitis the affected testis and epididymis demonstrate asymmetric and sometimes strikingly increased flow on Doppler ultrasound (Fig. 6-44A, B). Gray-scale ultrasound demonstrates enlargement and decreased echogenicity of the testis and epididymis. Reactive hydroceles are common.

Another cause of acute scrotum is torsion of the testicular appendage, a vestigial remnant of the mesonephric ducts. A mass of increased

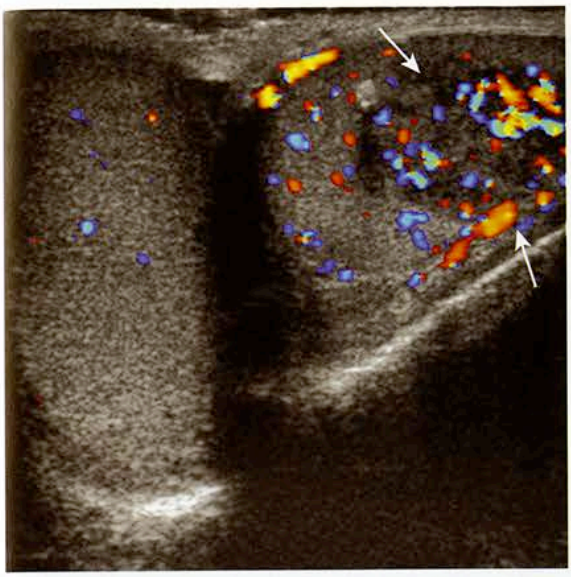

FIGURE 6-41. Testicular germ cell neoplasm. Transverse ultrasound shows focal, heterogeneous, hypoechogenic mass *(arrows)* in left testicle. Increased blood flow is shown on color Doppler.

echogenicity may be seen between the superior pole of the testis and the epididymis. Enlargement of the testicular appendage to greater than 5 mm has been touted as the best indicator of torsion. Periappendiceal hyperemia and normal testicular flow are supportive findings (Fig. 6-45A, B). Torsion of the testicular appendage is a self-limited entity and does not require surgical management. The importance of making the diagnosis is to avoid unnecessary surgical exploration.

FIGURE 6-42. Testicular microlithiasis. Longitudinal ultrasound of the left testicle shows multiple punctate areas of increased echogenicity without posterior shadowing.

Trauma may result in a testicular hematoma. On ultrasound, hematomas appear as avascular masses of abnormal echogenicity. Associated hematoceles are common.

ACUTE PELVIC PAIN IN OLDER GIRLS AND ADOLESCENTS

Acute pelvic pain in older girls and adolescents is a commonly encountered problem that has many possible causes. Pain can be related to menstruation, multiple ovarian pathologies, or appendicitis. Ovarian causes of pain include ovarian cysts, hemorrhagic cysts, ectopic pregnancy, ovarian torsion, endometriosis, pelvic inflammatory disease, or other masses such as teratoma (Fig. 6-46A, B) or other neoplasms (Fig. 6-47A, B). Ovarian dermoids (mature teratoma) can show fluid/fluid levels, fat, and calcifications on imaging (see Fig. 6-46). Other ovarian neoplasms are usually large at the time of presentation (see Fig. 6-47), can have a cystic or solid appearance, and typically do not have differentiating features at imaging. In girls with right lower quadrant pain, appendicitis is also a possibility. The high incidence and variety of pathologic processes that may involve the ovaries make ultrasound the primary imaging modality for right lower quadrant pain in girls.

Hemorrhagic cysts are a common cause of pelvic pain in adolescent girls. On ultrasound, the lesions appear as echogenic masses that often have enhanced through-transmission. Sometimes the masses can be quite large. Ovarian cysts can be discovered when CT is performed to evaluate for appendicitis (Fig. 6-48).

Ovarian torsion, which is less common than hemorrhagic cysts, can appear as an enlarged and echogenic ovary secondary to edema. There can be prominent peripheral follicular cysts, which are highly suggestive of the diagnosis (Figs. 6-49A, B, 6-50). However, the most commonly encountered positive finding is asymmetric ovarian volumes, with the larger ovary located on the side of pain. Doppler ultrasound demonstration of decreased or absent blood flow has not been shown to be accurate in diagnosing or excluding ovarian torsion. Note that a hemorrhagic cyst compressing the ovarian parenchyma peripherally can have a similar appearance and at times cannot be differentiated from ovarian torsion.

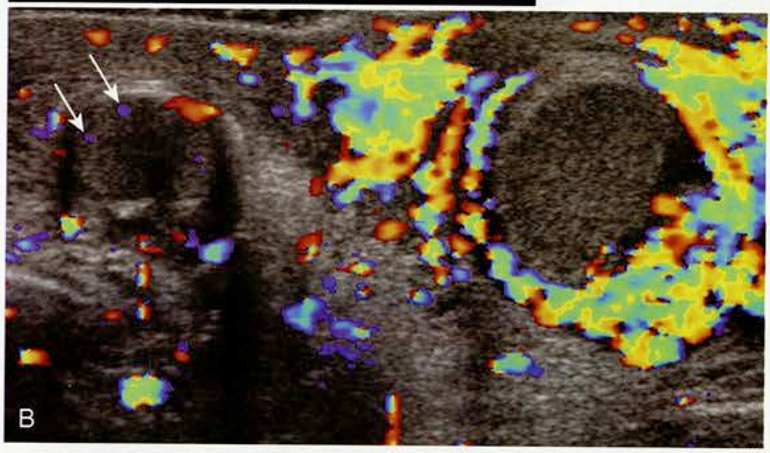

FIGURE 6-43. Testicular torsion, two examples. **A,** Transverse Doppler ultrasound showing both testes in a boy with left scrotal pain demonstrates absent flow and heterogeneous echo-texture of left testicle *(arrows).* Note normal echo-texture and present flow on right. **B,** Later findings of torsion in different patient. Transverse Doppler ultrasound showing both testes in boy with left scrotal pain demonstrates absent flow and heterogeneous echo-texture of left testicle. Note the flow detected *(arrows)* in the right testicle. There is a large amount of flow surrounding the left testicle, related to inflammatory reaction secondary to the necrosis.

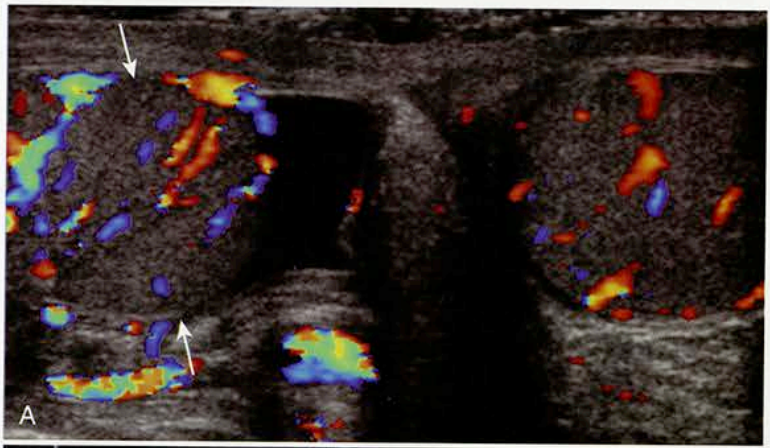

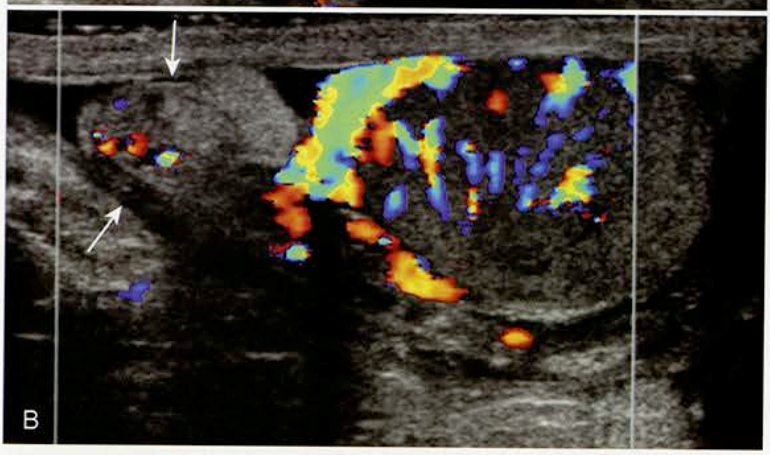

FIGURE 6-44. Epidydimoorchitis in a boy with acute onset of right scrotal pain. **A,** Transverse color Doppler ultrasound shows asymmetric increased flow to the symptomatic right testis *(arrows).* There is a reactive hydrocele. **B,** Longitudinal color Doppler ultrasound shows enlarged epidydimis *(arrows).* There is increased flow to both the epidydimis and the testicle.

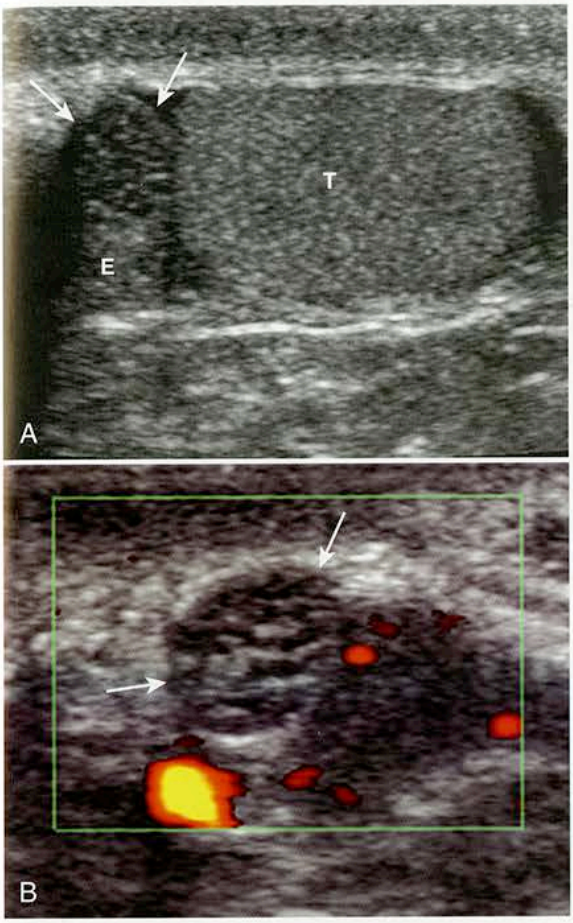

FIGURE 6-45. Torsion of the testicular appendage. **A,** Longitudinal view of the symptomatic side shows testicular appendage *(arrows)* to be enlarged (>5 mm). The appendage sits between the testicle *(T)* and the epididymis *(E).* **B,** Color Doppler ultrasound image shows absence of flow to the testicular appendage *(arrows).*

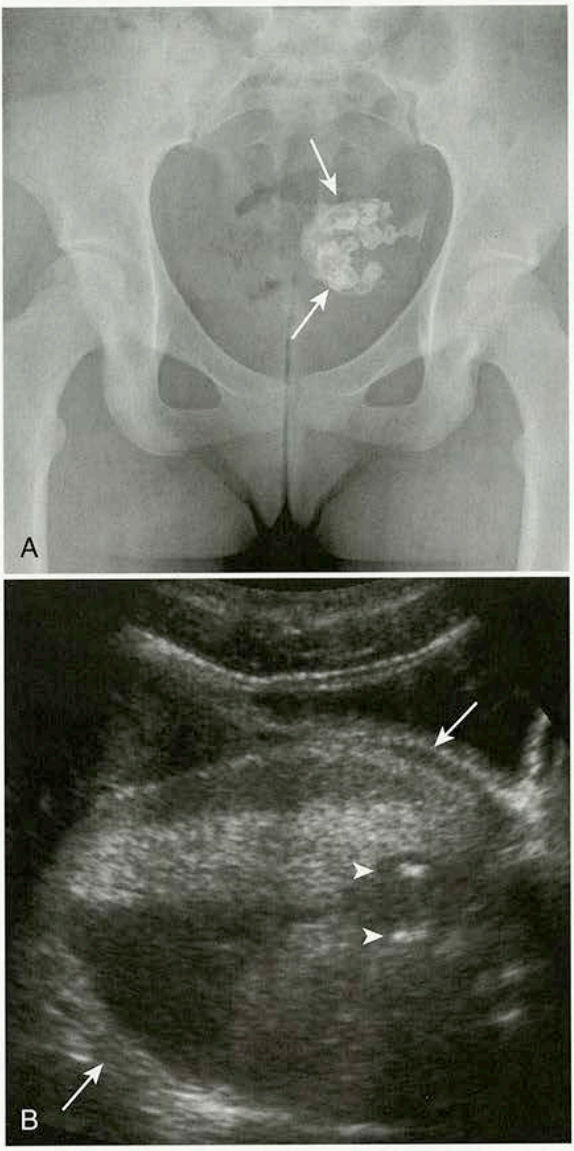

FIGURE 6-46. Ovarian dermoid (mature teratoma). **A,** Radiograph shows cluster of well-developed teeth in the pelvis *(arrows).* **B,** Ultrasound demonstrates mass in left ovary *(arrows)* with fluid-fluid levels of various echogenicities. Note echogenic teeth *(arrowheads).*

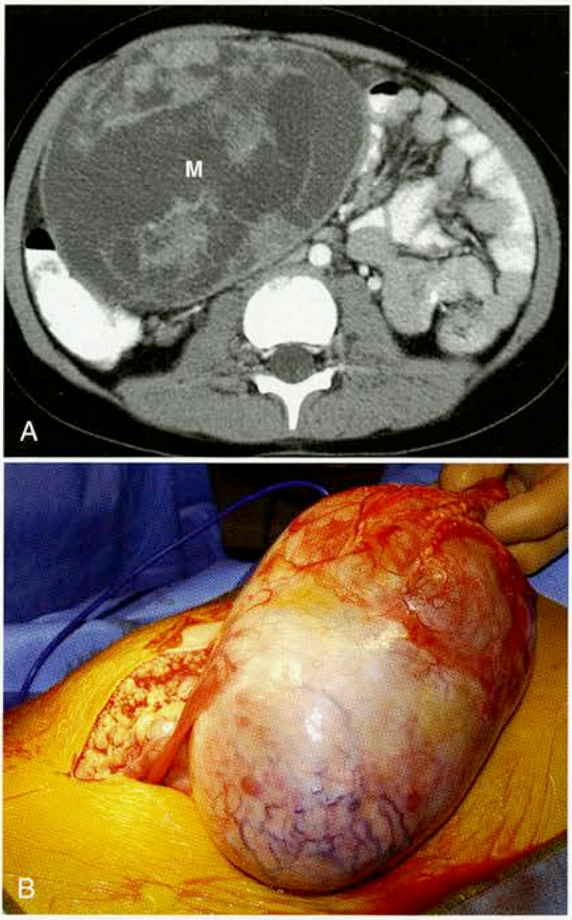

FIGURE 6-47. Sertoli cell neoplasm of the ovary. **A,** CT shows heterogeneous mass arising from right superior pelvis *(M).* **B,** Surgical photograph shows large mass arising from right ovary.

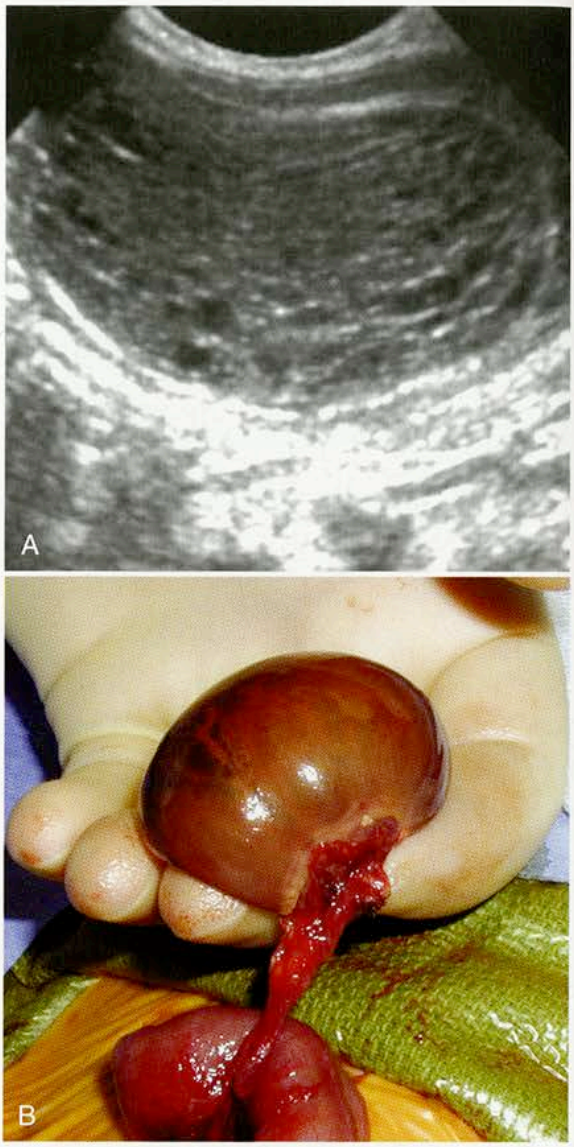

FIGURE 6-49. Ovarian torsion. **A,** Ultrasound shows asymmetrically enlarged ovary with increased echogenicity and some peripheral cysts. Doppler evaluation (not shown) showed no vascular flow. **B,** Surgical photograph showing infarcted ovary.

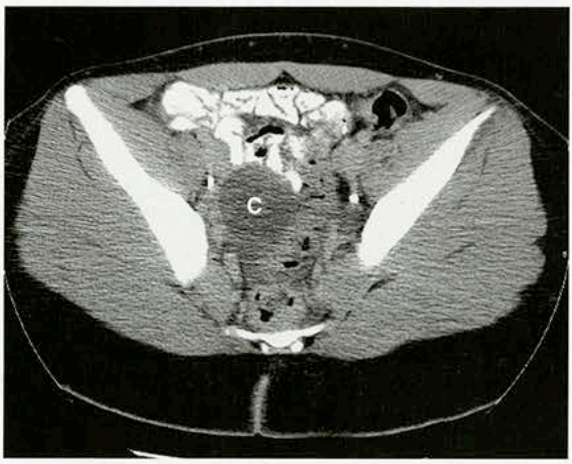

FIGURE 6-48. Hemorrhagic cyst identified on CT in a 14-year-old obese girl with right lower quadrant pain and suspected appendicitis. CT shows 5-cm cyst *(C)* in region of right adenexa.

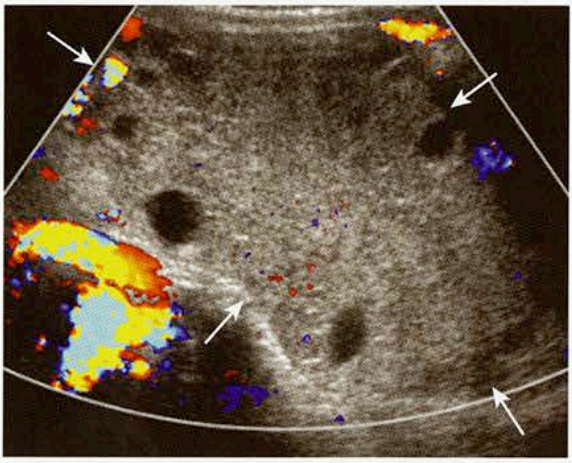

FIGURE 6-50. Ovarian torsion. Ultrasound shows asymmetrically enlarged ovary *(arrows)* with increased echogenicity and peripheral cysts. Doppler evaluation shows no vascular flow to ovary.

Suggested Readings

Daneman A, Alton DJ: Radiographic manifestations of renal anomalies, *Radiol Clin North Am* 29:351-363, 1991.

Frush DP, Sheldon CA: Diagnostic imaging of pediatric scrotal disorders, *Radiographics* 18:969-985, 1998.

Han BK, Babcock DS: Sonographic measurements and appearance of normal kidneys in children, *AJR* 145: 611-618, 1985.

Hartman DS: Renal cystic disease in multisystem conditions, *Urol Radiol* 14:13-17, 1992.

Kirks DR, Kaufman RA, Babcock DS: Renal neoplasms in infants and children, *Semin Roentgenol* 22:292-302, 1987.

Kraus SJ: Genitourinary imaging in children. *Pediatr Clin North Am* 48:1381-1424, 2001.

Lebowitz RL, Olbing H, Parkkulainen KV, et al: International system of radiographic grading of vesicoureteral reflux: International reflux study in children, *Pediatr Radiol* 15:105-109, 1985.

Ng YY, Kingston JE: The role of radiology in the staging of neuroblastoma, *Clin Radiol* 47:226-235, 1993.

Sty JR, Wells RY, Schroeder BA, Starshak RJ: Diagnostic imaging in pediatric renal inflammatory disease, *JAMA* 256:895-899, 1986.